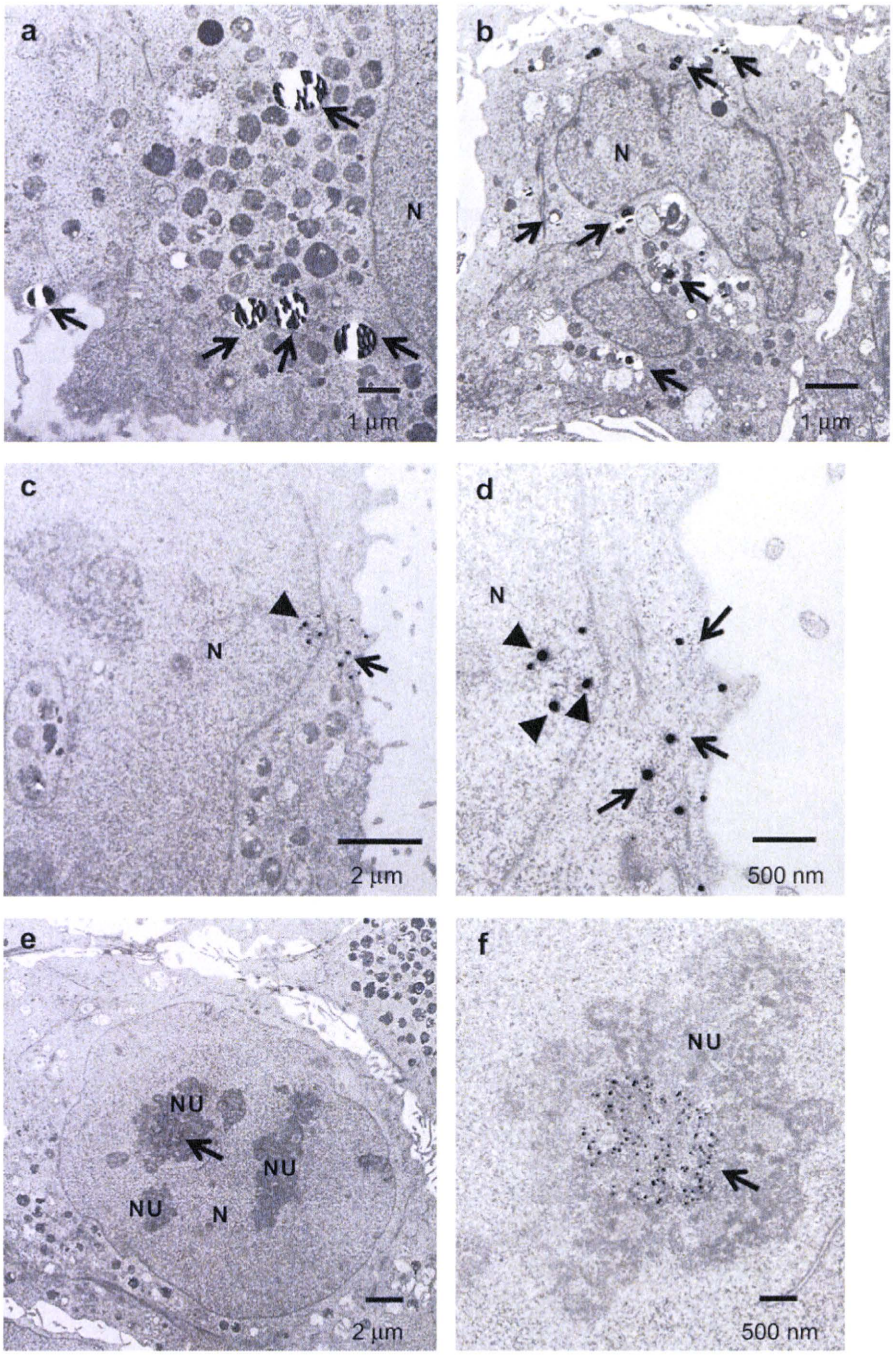

Fig. 4. TEM analysis of HaCaT cells treated with silica particles. a–e, Silica particles (arrows) were found in HaCaT cells treated for 24 h with 100 μg/ml of mSP1000 (a), nSP300 (b), and nSP70 (c, d, and e). In panels c and d, arrow heads show the presence of nSP70 in the nucleus, and in panels e and f, arrows show the presence of nSP70 in the nucleolus. Panels d and f are same as panels c and e at higher magnifications, respectively. N: nucleus; NU: nucleolus. Scale bars: 1 μm (a and b), 2 μm (c and e) and 500 nm (d and f).

concentrations (particles/ml) (Fig. 5b). This result suggested that the biological effects of NMs were different by material.

On the basis of the nuclear entry of nSP70 *in vivo* and *in vitro*, we next evaluated the mutagenicity of silica particles using *S. typhimurium* strains TA98 and TA100 (Ames test). None of the nSP that we tested induced mutation in TA98 strain when used at the indicated concentrations (Fig. 6a). By contrast, nSP of all sizes induced mutagenicity in TA100 strain at the highest dose of treatment (810 μg/ml) (Fig. 6b). At lower doses (30 and 90 μg/ml) of treatment, only nSP70 induced mutation in TA100 strain (Fig. 6b). Thus, the results obtained from the Ames test suggest that the mutagenicity of the silica particles increased with the decreasing particle size. Next, we used the comet assay to analyze DNA single strand breaks in nSP-treated HaCaT cells. In cells treated with PBS (negative control) for 3 h, the average tail length was 23.3 μm (Fig. 6c). In cells treated with 90 μg/ml of nSP70, nSP100, nSP300, or mSP1000, the average tail lengths were 102.9 μm (Fig. 6d), 88.8 μm (data not shown), 30.5 μm (Fig. 6e), and 22.5 μm (Fig. 6f), respectively.

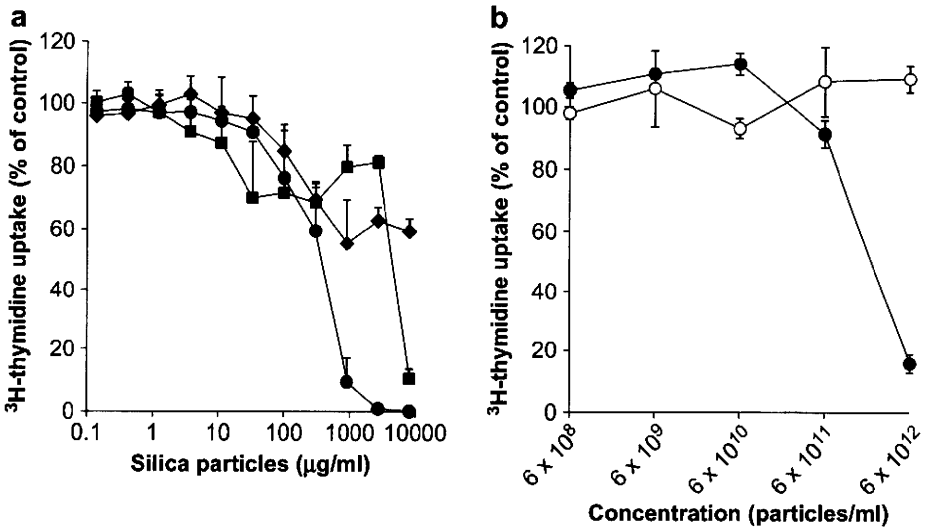

Fig. 5. Effect of various sized silica particles and QDs on cell proliferation. a) In order to assess the biological effects according to particle size, proliferation of HaCaT cells following 24 h of incubation with the indicated concentrations of nSP70 (closed circle), nSP300 (closed square) and mSP1000 (closed diamond) were measured using the tritium thymidine uptake assay. b) In order to assess the biological effects according to the material, proliferation of HaCaT cells following 24 h of incubation with the indicated concentrations of nSP70 (closed circle) and QD (opened circle) were measured. Results shown as relative rates (% of control). Each data point represents mean ± SD (n = 3).

The average tail lengths increased depending on the dose and size of the silica particles (Fig. 6g). The tail lengths found in the nSP70- and nSP100-treated cells were longer than those found in the positive control cells (0.2 mM H_2O_2 treated cells). These findings suggest the possibility that nSP with particle sizes below 100 nm could induce mutation.

3.6. Analysis of in vivo biodistribution of silica particles in mice

We next analyzed biodistribution and biological effects in systemic level using silica particles-injected mice, because it was suggested that nSP moved to the blood stream from skin as described above. To elucidate the *in vivo* distribution of silica particles, we determined the distribution of silica particles following intravenous injection, by optical imaging analysis (Fig. 7a–c). Intense fluorescence was observed near the liver in all silica particle-treated mice immediately after treatment and this signal migrated to near the intestinal tract with time. Imaging of dissected liver from nSP300- or mSP1000-treated mice revealed that intense fluorescence was observed only around the gall bladder. In contrast, nSP70-derived fluorescence was observed throughout dissected liver. In addition, our preliminary results revealed that all silica particle-derived fluorescence was also observed in intestinal tract and feces (data not shown), suggesting that silica particles might be excreted in the bile after circulating systemically, in a manner independent of particle size.

To clarify detailed localization of silica particles in liver of nSP-injected mice, next we perform transmission electron microscopy (TEM) analysis (Fig. 7d–g). While silica particles of all sizes were found to be ingested into Kupffer cells, nSP70 and nSP300 were also observed in parenchymal hepatocytes. In the nSP70-treated group, particles were shown to be localized in the cytoplasm and nucleus of various tissues such as lung, kidney, spleen and lymph node (data not shown). Microscopic findings showed that with reduction in particle size, silica particle uptake into Kupffer cells tended to be decreased and in contrast, particle uptake into the cytoplasm of parenchymal hepatocytes tended to be increased (Fig. 7h). Surprisingly, sub-nuclear localization of particles was observed in nSP70-treated groups (Fig. 7e). These results confirmed that the distribution of nSPs with particle size less than 100 nm differ from those of submicron-sized silica particles. These data strongly suggested that we must distinguish nSPs from existing submicron-sized silica particles, and address specialized risk assessment for nSPs.

3.7. Analysis of cytotoxicity and genotoxicity in primary hepatocyte induced by silica particles

Subsequently, we confirmed whether the biological effects induced by nSP in liver in which silica particles accumulated. The liver is one of the most important tissue in the body, because the liver takes an important role in metabolism, discharge, detoxification, maintenance of homeostasis of the body fluid. Especially, hepatocyte plays a vital role as functions of the liver. Using primary hepatocyte isolated from silica particles-injected mice intravenously, cytotoxicity and DNA damage of hepatocyte were analyzed. As the result, cytotoxicity of hepatocyte from nSP300 and mSP1000-injected mice little occurred. On the other hand, hepatocyte from nSP70-injected mice indicated higher cytotoxicity than nSP300 and mSP1000-injected mice (Fig. 8a). Furthermore, DNA damage of hepatocyte was detected only in nSP70-injected mice as well as in HaCaT cells (Fig. 8b). These results also indicate that differences in biological effects such as cytotoxicity and genotoxicity are caused by differences in biodistribution of silica particles. And it suggests that accumulation of nSP into the liver and/or nucleus may lead to genotoxicity.

Thus, we also highly recommend including carcinogenicity test and reproductive and developmental toxicity test for ensuring biosafety of NMs. Additionally, because nSP70 were accumulated in the nucleus, we suggest evaluating the effect of an NM on protein synthesis to further ensure its biosafety.

Nuclear pores are made of large protein complexes that cross the nuclear envelope, the membrane bilayer that surrounds the nucleus of the eukaryotic cell, and the pores are about 30 nm in diameter [31,32]. Thus, it is unlikely that the nSP70, which has a mean diameter of about 70 nm, entered the nucleus through the nuclear pore. We hypothesize that the nSP70 might interact with the nuclear transporting proteins via specific- or non-specific

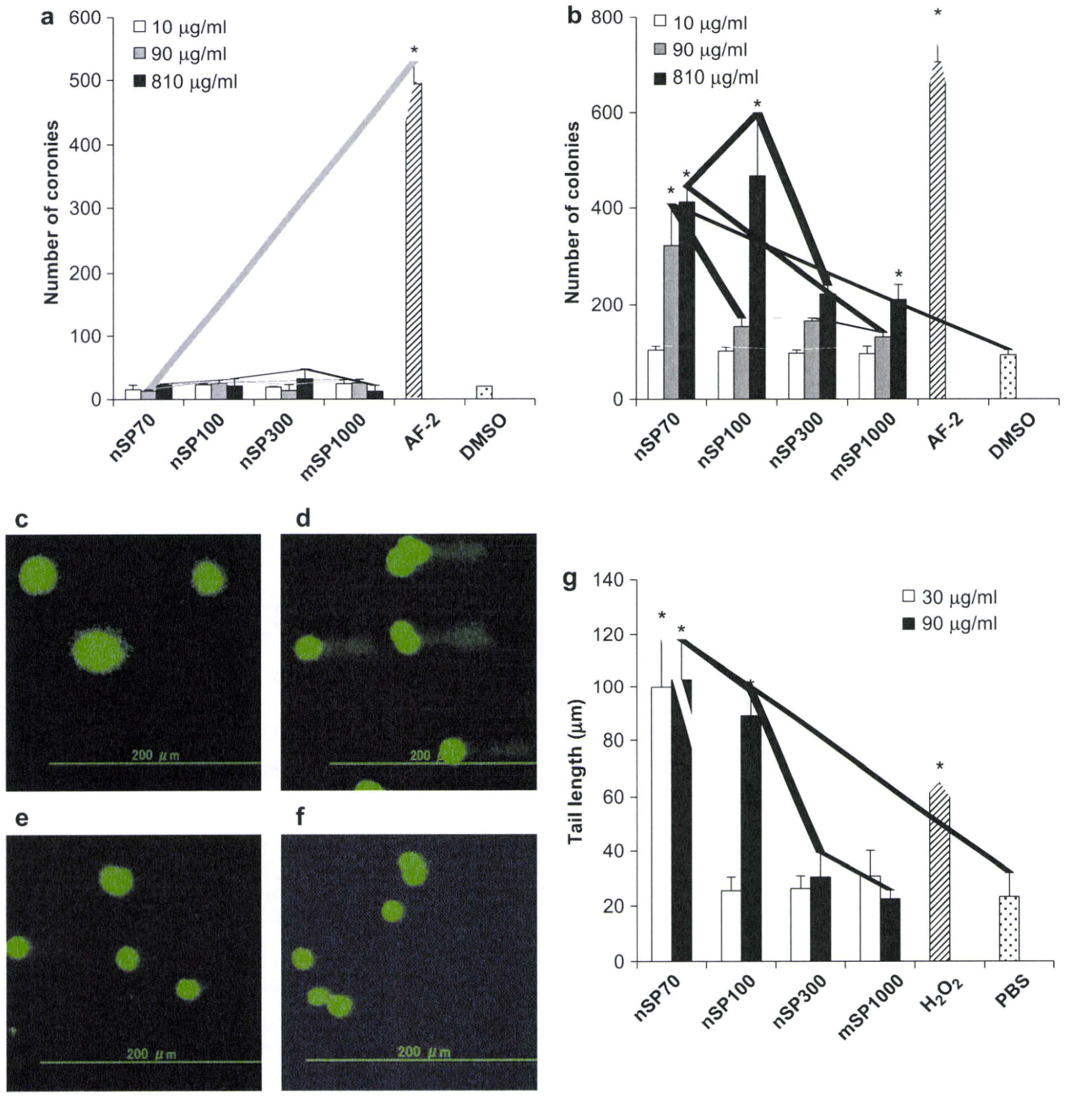

Fig. 6. Genotoxic effects of silica particles. a–b, Mutagenic effects of silica particles as determined by the Ames test. Dose-response of mutagenic effects of nSP70, nSP300, and mSP1000 on *S. typhimurium* strains: strain TA98 (a) and strain TA100 (b). The Ames test was performed as described in Methods. Values shown are mean ± SD ($n = 3$). *More than 2-fold increase compared to the medium-treated control (DMSO). AF-2, positive control. e–g, Detection of DNA strand breaks by the comet assay. Representative fluorescence images of HaCaT cells treated for 3 h with PBS (negative control) (c), or 90 μg/ml of nSP70 (d), nSP300 (e), and mSP1000 (f). Scale bar: 200 μm e, Column graph showing the tail lengths after being incubated with 30 μg/ml (open column) and 90 μg/ml (closed column), respectively, of nSP70, nSP300, and mSP1000, and 0.2 mM H_2O_2 (positive control) for 3 h. Data shown are average means (±SD) of at least 16 cells for each sample. Results shown are representative of more than three independent experiments. *Significant increase ($P < 0.01$) compared with the negative control, PBS.

interactions, and the nSP70/protein complexes are then transported into the nucleus. To test this hypothesis, we are currently pursuing a proteome-based approach to identify nSP70-interacting proteins.

Recently, commercially available amorphous silica-based products were subjected to various toxicological tests including acute and repeated dose toxicity, genotoxicity, carcinogenicity and reproductive toxicity [33]. According to this report, amorphous silica particles are non-toxic. Although the primary particle sizes of the amorphous silica used in these toxicological studies were between 1 and 100 nm, the ECETOC 2006 report stated that they did not exist as primary particles, but existed only as aggregates of particle sizes between 100 nm and 1 μm. The ECETOC 2006 report, however, did not exclude the possibility that materials having particle sizes below 100 nm might be developed and available for use in the future. In contrast to the results described in the ECETOC report, results of our present

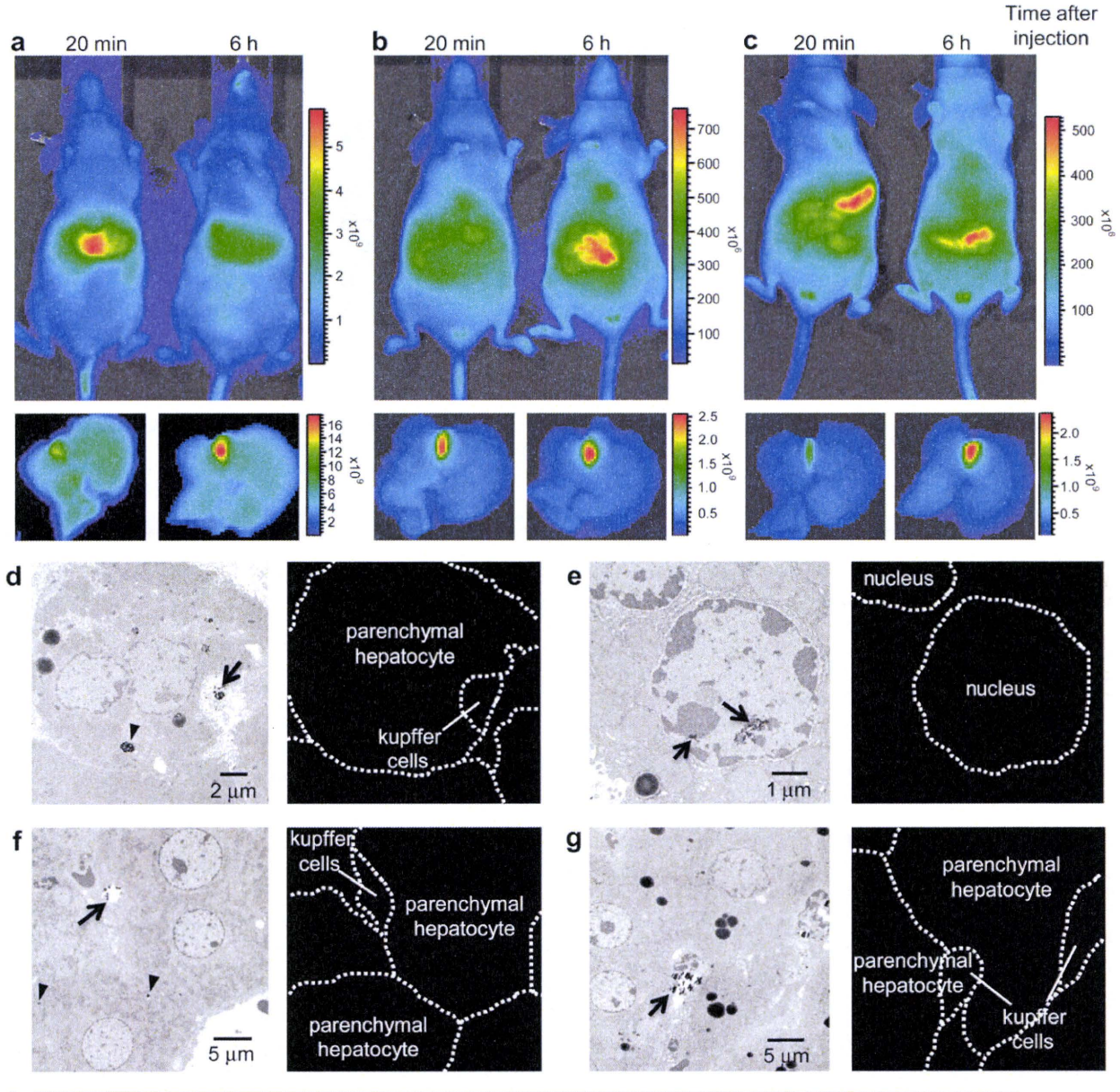

h

	nSP70	nSP300	mSP1000
Englobement in Kupffer cell	++	++	+++
Localization in cytoplasm of hepatocyte	+++	+	-
Localization in nucleus of hepatocyte	+	-	-

Fig. 7. Biodistribution analysis of silica particles at macro- and micro levels. A–C, Macro level analysis: optical imaging of fluorescently labeled silica particles in live mice and excised liver. DY676-labeled silica particles (a, nSP70, b, nSP300 and c, mSP1000, 100 mg/kg) were intravenously injected into female hairless mice. Twenty min and 6 h after injection, optical images were acquired using a Xenogen IVIS 200 imaging system. The signal intensity in the region of interest is expressed as photons (p) per second (sec) per centimeter squared (cm^2) per steradian (sr) (a steradian is a unit of solid angle). d–f, Micro level analysis: BALB/c mouse liver injected with 30 mg/kg (nSP70) or 100 mg/kg (nSP300 and mSP1000) nSPs was observed by TEM. d, arrow, nSP70, f arrow, nSP300, g, mSP1000 were phagocytosed in Kupffer cells. d, arrow head, nSP70 and f, arrow head, nSP300 were also detected in cytoplasm of parenchymal hepatocytes. Interestingly, e, nSP70 entered the nucleus of the parenchymal hepatocytes. Arrows and arrow heads indicate silica particles. Scale bar, d, 2 μm, e, 1 μm and f, g, 5 μm. H, Localization of each silica particle in liver is summarized. Amount of silica particles were shown as follows; −: Not detected, +: small, ++: middle, +++: large.

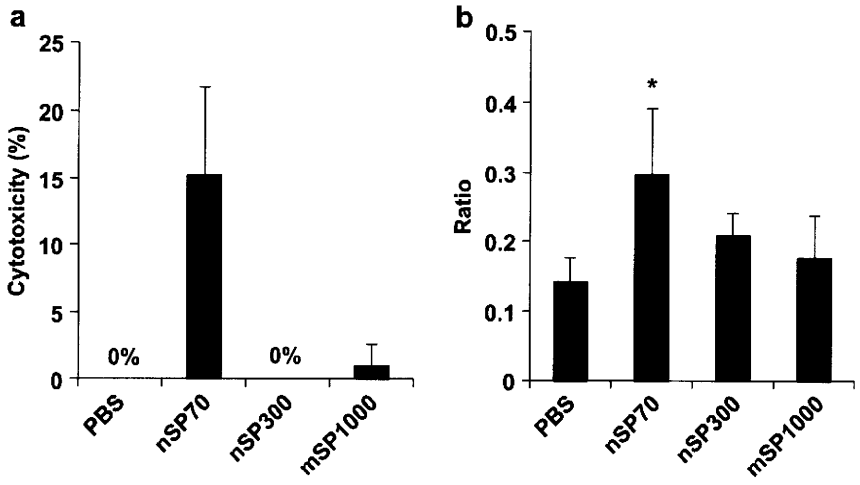

Fig. 8. Liver toxicity analysis in parenchymal hepatocytes. a, Cytotoxicity of parenchymal hepatocytes isolated from nSP-injected mice 5 h after injection by trypan blue stain. b, Detection of DNA strand breaks ratio of parenchymal hepatocytes isolated from nSP-injected mice 5 h after injection. Data are shown as mean ± SD; comet tails from at least 16 cells were counted in each sample. All data are representative of more than three slides. * Represents significant difference from the control group ($P < 0.01$).

study showed that well-dispersed nSP70 could indeed penetrate the skin barrier and cause systemic exposure, thus suggesting that the well-dispersed NMs have to be viewed as new entities and tested accordingly for ensuring their biosafety. It is known that the asbestos-related health hazard, symptoms of mesothelioma, appears after prolonged exposure to asbestos particles (average of 40 years, shortest around 20 years) [34–37]. Because of this and also in view of the growing demand for the NMs in various fields, there is a clear and urgent need for in depth risk assessment of all NMs for safety use. Keeping in line with this idea and because it is not known whether exposure to NMs might cause initiation and/or progression of various diseases (e.g., atopic dermatitis, infectious disease, etc.), we have initiated more detailed and extensive safety analysis studies including relationships between the physicochemical properties (i.e., size, shape, and surface property) of an NM and its biodistribution, and analysis of the interaction of the NMs with allergens, gastrointestinal flora, and resident floras as contributing factors to human health in order to further ensure its biosafety.

4. Conclusions

This study revealed that, as compared with the bulk material of particle sizes above nanoscale (above 100 nm), well-dispersed amorphous nanosilica with a particle size of 70 nm shows different bio-properties with respect to skin penetration and nuclear entry. These bio-properties of nanosilica show the potential as a new functional material, but, reflecting these differences, nSP70 exert various adverse biological effects in regional and systemic level, such as DNA fragmentation. We consider that more information which provided by further studies of relation between physicochemical properties and biological responses, would lead to realization of an affluent society by the use of safe and useful NMs.

Acknowledgments

This study was supported in part by Grants-in-Aid for Scientific Research from the Ministry of Education, Culture, Sports, Science and Technology of Japan, and from the Japan Society for the Promotion of Science (JSPS). This study was also supported in part by Health Labour Sciences Research Grants from the Ministry of Health, Labor and Welfare of Japan; by a Global Environment Research Fund from Ministry of the Environment; and by the Knowledge Cluster Initiative; and by The Nagai Foundation Tokyo; and by The Cosmetology Research Foundation; and by The Smoking Research Foundation.

References

[1] Salata O. Applications of nanoparticles in biology and medicine. J Nanobiotechnology 2004;2(1):3.
[2] Aiso S, Yamazaki K, Umeda Y, Asakura M, Takaya M, Toya T, et al. Pulmonary toxicity of intratracheally instilled multiwall carbon nanotubes in male Fischer 344 rats. Ind Health; 2010 [Epub ahead of print].
[3] Chen J, Dong X, Zhao J, Tang G. *In vivo* acute toxicity of titanium dioxide nanoparticles to mice after intraperitoneal injection. J Appl Toxicol 2009;29(4):330–7.
[4] Geys J, Nemmar A, Verbeken E, Smolders E, Ratoi M, Hoylaerts MF, et al. Acute toxicity and prothrombotic effects of quantum dots: impact of surface charge. Environ Health Perspect 2008;116(12):1607–13.
[5] Heng BC, Zhao X, Xiong S, Ng KW, Boey FY, Loo JS. Toxicity of zinc oxide (ZnO) nanoparticles on human bronchial epithelial cells (BEAS-2B) is accentuated by oxidative stress. Food Chem Toxicol 2010;48(6):1762–6.
[6] Kocbek P, Teskac K, Kreft ME, Kristl J. Toxicological aspects of long-term treatment of keratinocytes with ZnO and TiO(2) nanoparticles. Small 2010; 6(17):1908–17.
[7] Liu S, Xu L, Zhang T, Ren G, Yang Z. Oxidative stress and apoptosis induced by nanosized titanium dioxide in PC12 cells. Toxicology 2010;267(1–3):172–7.
[8] Moos PJ, Chung K, Woessner D, Honeggar M, Cutler NS, Veranth JM. ZnO particulate matter requires cell contact for toxicity in human colon cancer cells. Chem Res Toxicol 2010;23(4):733–9.
[9] Murray AR, Kisin E, Leonard SS, Young SH, Kommineni C, Kagan VE, et al. Oxidative stress and inflammatory response in dermal toxicity of single-walled carbon nanotubes. Toxicology 2009;257(3):161–71.
[10] Park EJ, Kim H, Kim Y, Yi J, Choi K, Park K. Carbon fullerenes (C60s) can induce inflammatory responses in the lung of mice. Toxicol Appl Pharmacol 2010; 244(2):226–33.
[11] Poland CA, Duffin R, Kinloch I, Maynard A, Wallace WA, Seaton A, et al. Carbon nanotubes introduced into the abdominal cavity of mice show asbestos-like pathogenicity in a pilot study. Nat Nanotechnol 2008;3(7):423–8.
[12] Shin JA, Lee EJ, Seo SM, Kim HS, Kang JL, Park EM. Nanosized titanium dioxide enhanced inflammatory responses in the septic brain of mouse. Neuroscience 2010;165(2):445–54.
[13] Takagi A, Hirose A, Nishimura T, Fukumori N, Ogata A, Ohashi N, et al. Induction of mesothelioma in p53+/− mouse by intraperitoneal application of multi-wall carbon nanotube. J Toxicol Sci 2008;33(1):105–16.
[14] Yamashita K, Yoshioka Y, Higashisaka K, Morishita Y, Yoshida T, Fujimura M, et al. Carbon nanotubes elicit DNA damage and inflammatory response relative to their size and shape. Inflammation 2010;33(4):276–80.
[15] Nabeshi H, Yoshikawa T, Matsuyama K, Nakazato Y, Arimori A, Isobe M, et al. Size-dependent cytotoxic effects of amorphous silica nanoparticles on Langerhans cells. Pharmazie 2010;65(3):199–201.
[16] Singh S, Shi T, Duffin R, Albrecht C, van Berlo D, Hohr D, et al. Endocytosis, oxidative stress and IL-8 expression in human lung epithelial cells upon

treatment with fine and ultrafine TiO_2: role of the specific surface area and of surface methylation of the particles. Toxicol Appl Pharmacol 2007;222 (2):141–51.
[17] Thibodeau M, Giardina C, Hubbard AK. Silica-induced caspase activation in mouse alveolar macrophages is dependent upon mitochondrial integrity and aspartic proteolysis. Toxicol Sci 2003;76(1):91–101.
[18] Chlopek J, Czajkowaska B, Szaraniec B, Frackowiak E, Szostak K, Beguin F. *In vitro* studies of carbon nanotubes biocompatibility. Carbon 2006;44:1106–11.
[19] Bharali DJ, Klejbor I, Stachowiak EK, Dutta P, Roy I, Kaur N, et al. Organically modified silica nanoparticles: a nonviral vector for *in vivo* gene delivery and expression in the brain. Proc Natl Acad Sci U S A 2005;102(32):11539–44.
[20] Bottini M, D'Annibale F, Magrini A, Cerignoli F, Arimura Y, Dawson MI, et al. Quantum dot-doped silica nanoparticles as probes for targeting of T-lymphocytes. Int J Nanomedicine 2007;2(2):227–33.
[21] Hirsch LR, Stafford RJ, Bankson JA, Sershen SR, Rivera B, Price RE, et al. Nanoshell-mediated near-infrared thermal therapy of tumors under magnetic resonance guidance. Proc Natl Acad Sci U S A 2003;100(23):13549–54.
[22] Roy I, Ohulchanskyy TY, Bharali DJ, Pudavar HE, Mistretta RA, Kaur N, et al. Optical tracking of organically modified silica nanoparticles as DNA carriers: a nonviral, nanomedicine approach for gene delivery. Proc Natl Acad Sci U S A 2005;102(2):279–84.
[23] Verraedt E, Pendela M, Adams E, Hoogmartens J, Martens JA. Controlled release of chlorhexidine from amorphous microporous silica. J Control Release 2010;142(1):47–52.
[24] Ames BN, Gurney EG, Miller JA, Bartsch H. Carcinogens as frameshift mutagens: metabolites and derivatives of 2-acetylaminofluorene and other aromatic amine carcinogens. Proc Natl Acad Sci U S A 1972;69(11):3128–32.
[25] Ames BN, Durston WE, Yamasaki E, Lee FD. Carcinogens are mutagens: a simple test system combining liver homogenates for activation and bacteria for detection. Proc Natl Acad Sci U S A 1973;70(8):2281–5.
[26] McCann J, Spingarn NE, Kobori J, Ames BN. Detection of carcinogens as mutagens: bacterial tester strains with R factor plasmids. Proc Natl Acad Sci U S A 1975;72(3):979–83.
[27] Mortensen LJ, Oberdorster G, Pentland AP, Delouise LA. *In vivo* skin penetration of quantum dot nanoparticles in the murine model: the effect of UVR. Nano Lett 2008;8(9):2779–87.
[28] Nohynek GJ, Lademann J, Ribaud C, Roberts MS. Grey goo on the skin? Nanotechnology, cosmetic and sunscreen safety. Crit Rev Toxicol 2007;37(3): 251–77.
[29] Wolf R, Matz H, Orion E, Lipozencic J. Sunscreens–the ultimate cosmetic. Acta Dermatovenerol Croat 2003;11(3):158–62.
[30] AshaRani PV, Low Kah Mun G, Hande MP, Valiyaveettil S. Cytotoxicity and genotoxicity of silver nanoparticles in human cells. ACS Nano 2009;3(2): 279–90.
[31] Akey CW. Interactions and structure of the nuclear pore complex revealed by cryo-electron microscopy. J Cell Biol 1989;109(3):955–70.
[32] Reichelt R, Holzenburg A, Buhle Jr EL, Jarnik M, Engel A, Aebi U. Correlation between structure and mass distribution of the nuclear pore complex and of distinct pore complex components. J Cell Biol 1990;110(4):883–94.
[33] European Centre for Ecotoxicology and Toxicology of Chemicals (ECETOC). Synthetic Amorphous Silica (CAS No. 7631-86-9). ECETOC JACC Report No.51; 2006.
[34] Enterline PE, Henderson V. Type of asbestos and respiratory cancer in the asbestos industry. Arch Environ Health 1973;27(5):312–7.
[35] Luo S, Liu X, Mu S, Tsai SP, Wen CP. Asbestos related diseases from environmental exposure to crocidolite in Da-yao, China. I. Review of exposure and epidemiological data. Occup Environ Med 2003;60(1):35–42.
[36] McDonald JC, McDonald AD. The epidemiology of mesothelioma in historical context. Eur Respir J 1996;9(9):1932–42.
[37] Selikoff IJ, Lilis R, Nicholson WJ. Asbestos disease in United States shipyards. Ann N Y Acad Sci 1979;330:295–311.

Nabeshi et al. Particle and Fibre Toxicology 2011, 8:1
http://www.particleandfibretoxicology.com/content/8/1/1

PARTICLE AND FIBRE TOXICOLOGY

RESEARCH Open Access

Amorphous nanosilica induce endocytosis-dependent ROS generation and DNA damage in human keratinocytes

Hiromi Nabeshi[1,2], Tomoaki Yoshikawa[1,2*], Keigo Matsuyama[1,2], Yasutaro Nakazato[1,2], Saeko Tochigi[1,2], Sayuri Kondoh[1,2], Toshiro Hirai[1,2], Takanori Akase[1,2], Kazuya Nagano[2], Yasuhiro Abe[2], Yasuo Yoshioka[2,3], Haruhiko Kamada[2,3], Norio Itoh[1], Shin-ichi Tsunoda[1,2,3], Yasuo Tsutsumi[1,2,3*]

Abstract

Background: Clarifying the physicochemical properties of nanomaterials is crucial for hazard assessment and the safe application of these substances. With this in mind, we analyzed the relationship between particle size and the *in vitro* effect of amorphous nanosilica (nSP). Specifically, we evaluated the relationship between particle size of nSP and the *in vitro* biological effects using human keratinocyte cells (HaCaT).

Results: Our results indicate that exposure to nSP of 70 nm diameter (nSP70) induced an elevated level of reactive oxygen species (ROS), leading to DNA damage. A markedly reduced response was observed using submicron-sized silica particles of 300 and 1000 nm diameter. In addition, cytochalasin D-treatment reduced nSP70-mediated ROS generation and DNA damage, suggesting that endocytosis is involved in nSP70-mediated cellular effects.

Conclusions: Thus, particle size affects amorphous silica-induced ROS generation and DNA damage of HaCaT cells. We believe clarification of the endocytosis pathway of nSP will provide useful information for hazard assessment as well as the design of safer forms of nSPs.

Background

With recent developments in nanotechnology, various kinds of nanomaterials have been designed and produced throughout the world. Nanomaterials have been widely used in consumer and industrial applications, such as medicine, cosmetics and foods, because they exhibit unique physicochemical properties and innovative functions [1]. For example, materials such as amorphous silica nanoparticles (nSPs) and titanium dioxide (TiO_2) are colorless and reflect ultraviolet light more efficiently than micro-sized particles. Consequently, these substances are already used as functional ingredients in many cosmetics such as foundation creams and sunscreens.

However, concerns over the potentially harmful effects of nanomaterials have been raised precisely because they possess novel properties that are different from those of microsized materials. Increasing numbers of studies show that many types of nanomaterials, such as carbon nanotubes, fullerenes, quantum dots, zinc oxide and TiO_2, have a harmful effect on cells and rodents [2-14]. For example, previous studies reported that various nanoparticles induced toxicological effects mainly in lung, liver, spleen and kidney tissues [3,10,15-19]. *In vivo* toxicity studies in Sprague Dawley rats showed that inhaled silver nanoparticles elicited chronic inflammation in the lungs [20]. After intravenous injection with silica nanoparticles in BALB/c mice, 70 nm particles induced liver injury at 30 mg/kg, while 300 nm or 1000 nm had no effect [21]. Recent evidence indicates that the small size and high surface area of nanomaterials may cause unpredictable genotoxic properties [22]. For example, induction of DNA damage by gold-, silver-, cobalt-, TiO_2-nanoparticles has been reported. The results from various studies suggest that these nanomaterials may cause DNA damage by an indirect pathway through promoting oxidative stress and inflammatory responses *via* dysfunction of

* Correspondence: tomoaki@phs.osaka-u.ac.jp; ytsutsumi@phs.osaka-u.ac.jp
[1]Graduate School of Pharmaceutical Sciences, Osaka University, 1-6 Yamadaoka, Suita, Osaka 565-0871, Japan
Full list of author information is available at the end of the article

mitochondria or inflammasomes. Central to the study of nanotoxicology is genotoxicity, the study of genetic aberrations following exposure to nanomaterials, because it is known that an increased genetic instability is associated with the development of cancer.

A sufficient understanding of the relationship between the physicochemical characteristics of nanomaterials governing their cytotoxicity (i.e. genotoxicity) and the identification of factors that influence their associated hazards are essential for the development of safer nanomaterials [22-25]. Since the linkage analysis is the sole methods for developing safe nanomaterials, many researchers have conducted extensive efforts [26-30]. In this context, the aim of our study was to investigate the relationship between particle size and in vitro hazard of amorphous nanosilica (nSP), especially focusing on DNA damage, using human keratinocyte cells.

Results and Discussion

We first analyzed the physicochemical properties of the commercially available silica particles of 70, 300 and 1000 nm in diameter (nSP70, nSP300 and mSP1000, respectively). Close examination of the silica particles of different particle sizes (nSP70, nSP300, mSP1000) by scanning electron microscopy (SEM) revealed that all the particles used in this study were spherical and the primary particle sizes were approximately uniform (Figure 1A-C). The size distribution spectrum of each set of silica particles in a neutral solvent showed a single peak. Moreover, the average particle size corresponded almost precisely to the anticipated size for each sample (Figure 1D and 1E). These results suggest that the silica particles used in this study remained as stable well-dispersed particles in solution.

Cosmetic products containing nSP, such as those used in skincare treatments, have been on the market

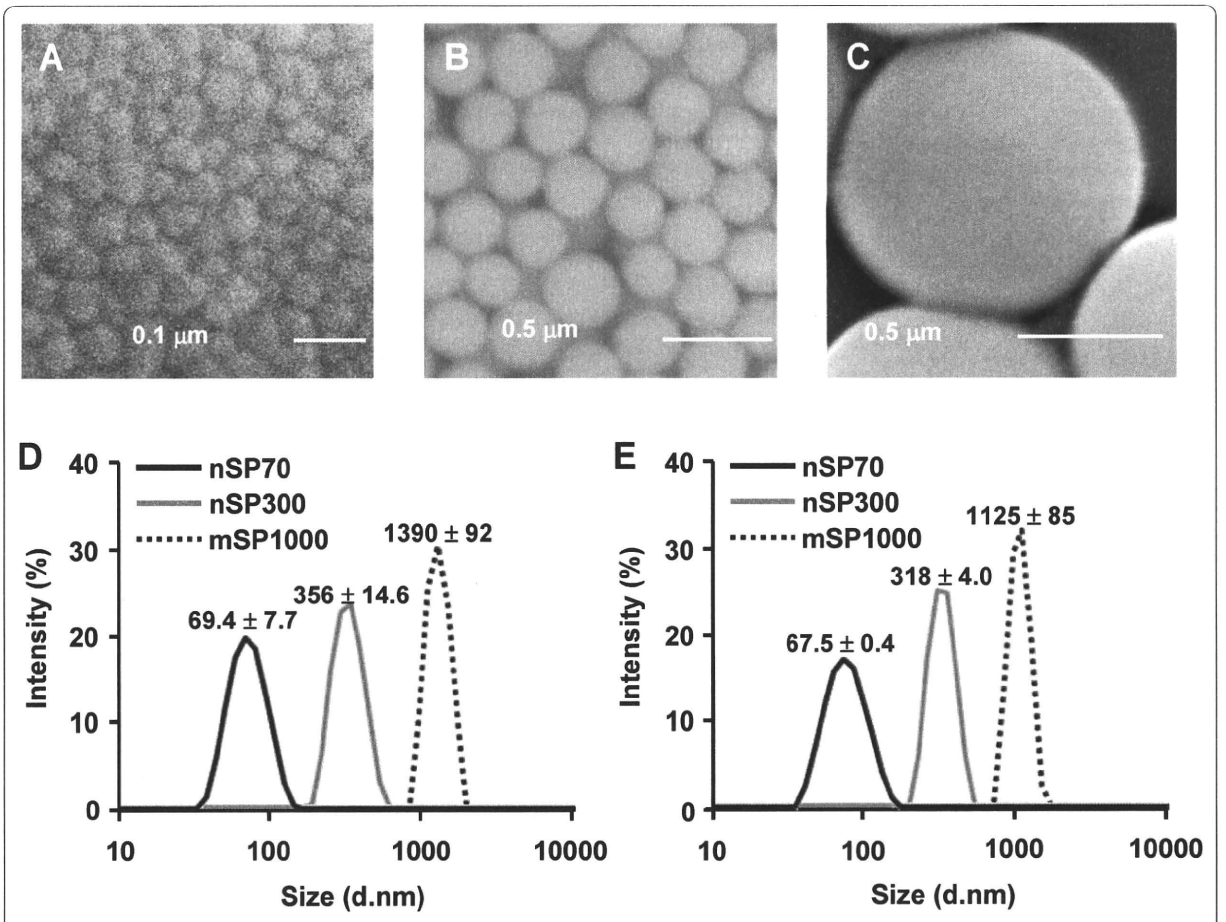

Figure 1 Scanning electron microscopy (SEM) analysis and spectrum of size distribution of amorphous silica particles. (A-C) SEM photomicrographs of silica particles used in this study: nSP70 (**A**), nSP300 (**B**) and mSP1000 (**C**). Scale bars: 0.1 mm (**A**) and 0.5 mm (**B and C**). **(D and E)** Size distribution of nSP70 (black), nSP300 (gray) and mSP1000 (dashed line) in water (**D**) or PBS (**E**) were measured by a dynamic light scattering method.

for a considerable period of time. Adult human skin has an average surface area of 1.95 m^2, weighs 3.18 kg and comprises over 300 million cells. The skin is the largest organ in the human body, which provides protection against heat, cold, electromagnetic radiation and chemical damage. Indeed, skin cells are likely to have the highest frequency of exposure to nSPs. Hence, a safety evaluation of nSPs using dermal cells is essential. Based on this consideration, using the HaCaT human keratinocyte cell line as a model system, we studied the effects of various sized silica particles on cell function. Specifically, we used HaCaT cells to perform the LDH release assay to assess membrane damage induced by silica particles. We found that membrane damage was not observed in nSP300- and mSP1000-treated HaCaT cells. By contrast, LDH release increased after exposure of the cells to nSP70 in a dose-dependent manner (Figure 2). This observation suggested that membrane damage in keratinocytes increased significantly when the particle size was less than 100 nm. The decrease of particle size changes the physicochemical properties of the silica particles, such as surface area and the number of functional groups per particle weight, which are both increased [31-34]. In addition, subsequent experiments were performed at a non-toxic dose (less than 300 μg/ml) in order to exclude the toxic effects of nSP70.

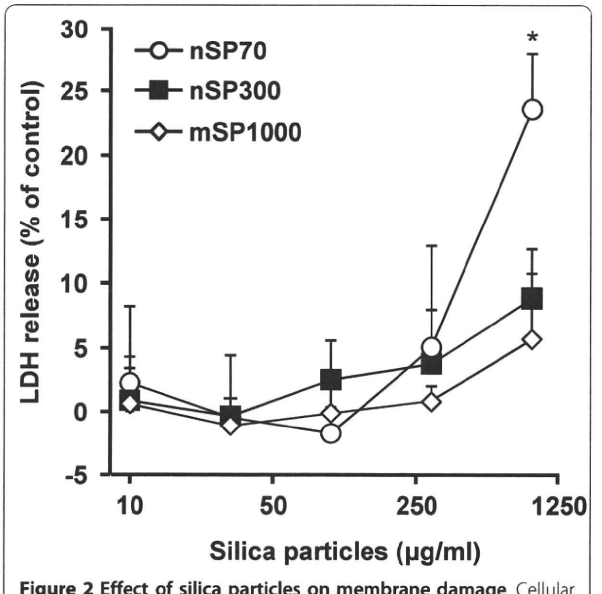

Figure 2 Effect of silica particles on membrane damage. Cellular membrane damage in HaCaT cells after incubation with nSP70 (circles), nSP300 (squares) and mSP1000 (diamonds) for 24 h was evaluated by the LDH release assay. The percentage cellular membrane damage was calculated relative to the negative (medium) controls. Data are presented as means ± SD (n = 3).*P < 0.01 vs same dose of nSP300 and mSP1000.

Some reports have indicated that intracellular generation of reactive oxygen species (ROS) is induced by nSP [35-37]. Furthermore, it has recently been reported that crystalline silica induces intracellular ROS generation *via* NADPH oxidase activation following uptake by endocytosis [38,39]. Based on these reports, ROS generation and DNA damage are an obvious means of assessing the hazard posed by nSP. Firstly, total intracellular ROS generation was measured in silica particle-treated HaCaT cells using 2'7'-dichlorodihydorofluorescein diacetate (DCFH-DA). Silica particles of all sizes were found to induce intracellular ROS generation in a dose-dependent fashion (Figure 3A). However, ROS generation by nSP70 treatment was significantly greater compared with nSP300 and mSP1000 treatment at the same particle concentration. Additionally, we confirmed that hydroxyl radicals, one of the most highly reactive ROS, were generated in HaCaT cells treated with silica particles, in particular with nSP70 (Figure 3B). Even in the 10 μg/ml-treated group, hydroxyl radical-generation effects of nSP70-treatment were 1.4 times higher than that of nSP300 and mSP1000-treated groups. These results suggested that silica particle-induced intracellular ROS generation was significantly increased by decreasing the particle size to less than 100 nm. ROS are defined as either "primary" or "secondary". Primary ROS (e.g. superoxide, O_2^-) can be generated through metabolic processes or through the activation of oxygen, which results in the formation of a reactive nucleophilic molecule of oxygen i.e., superoxide anion. These reactive species may interact with other molecules, such as redox active transition metals (e.g. iron) or enzymes, resulting in the production of "secondary" ROS (e.g. $^{\bullet}OH$), which are primary mediators of DNA damage. Consequently, we analyzed the formation of 7'8'-dihydro-8-oxodeoxyguanosine (8-OH-dG) as an indicator of ROS-induced DNA damage. When HaCaT cells were treated with various concentrations of silica particles for 3 h, 8-OH-dG levels in nSP300- and mSP1000-treated cells remained constant regardless of silica particle dose and were equal to the levels found in untreated cells (Figure 3C). By contrast, 8-OH-dG levels increased upon exposure of the cells to nSP70 in a dose-dependent manner. After treatment with nSP70 at 90 μg/ml the level of 8-OH-dG increased significantly compared with non-treated cells.

8-OH-dG is known as a major index of oxidative DNA damage related to mutagenesis, carcinogenesis and the aging process [40,41]. These reports, together with our results, suggest the possibility that nSP70 may be carcinogenic. Moreover, nSP-induced ROS may induce genotoxicity *via* DNA strand breaks, oxidative DNA damage and mutation. Indeed, DNA damage was detected in nSP70-treated HaCaT cells. In addition, nSP70-mediated DNA damage was inhibited by pre-treatment with the ROS scavenger, N-acetylcystein

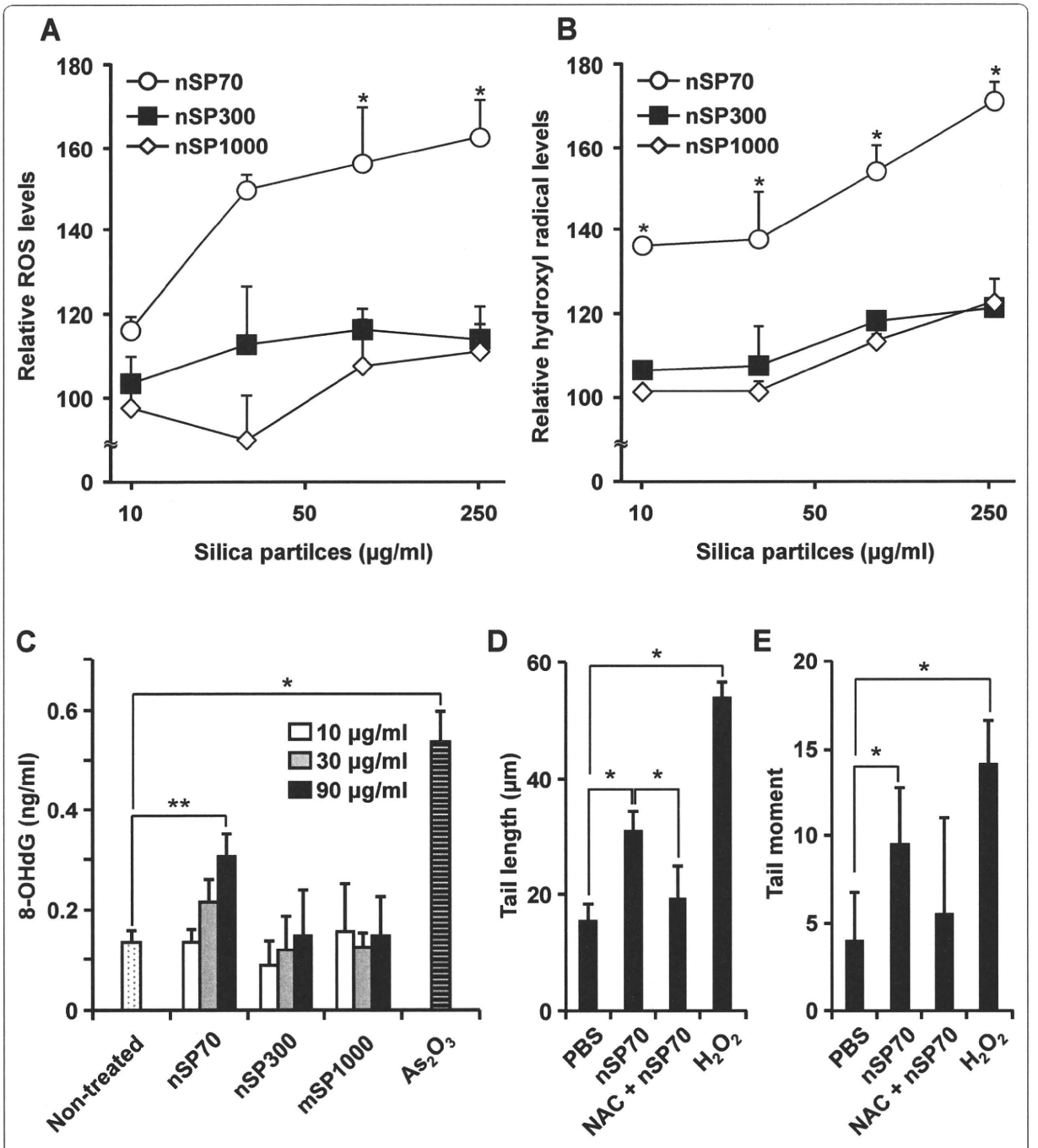

Figure 3 Detection of oxidative stress induced by silica particle treatment in HaCaT cells. Detection of total ROS and hydroxyl radical induced by silica particle treatment in HaCaT cells. HaCaT cells were incubated with various concentrations of nSP70 (circles), nSP300 (squares), and mSP1000 (diamonds) for 3 h. (**A**) Total ROS induced by treatment with silica particles were expressed as relative fluorescence units in the DCFH assay.*$P < 0.01$ vs same dose of nSP300 and mSP1000. (**B**) Hydroxyl radical was measured by hydroxyphenyl fluorescein (HPF) assay. Data shown are means ± SD (n = 3).*$P < 0.01$ vs same dose of nSP300 and mSP1000. (**C**) Detection of 8-OH-dG induced by silica particle treatment in HaCaT cells. HaCaT cells were incubated with 10, 30 or 90 mg/ml nSP70, nSP300, or mSP1000, and As_2O_3 (positive control) for 3 h. Data shown are means ± SD (n = 3). *$P < 0.01$, **$P < 0.05$. (**D and E**) Effects of ROS inhibitor on DNA strand breaks induced by silica particle treatment in HaCaT cells. HaCaT cells were pretreated with 2 mM N-acetylcystein (NAC) for 30 min (NAC + nSP70) or nSP70 alone, prior to incubation with 90 mg/ml nSP70 for 3 h. As a positive control, HaCaT cells were treated with 0.2 mM H_2O_2 for 3 h. (**D**) Column height shows the tail length. (**E**) Column height shows the tail moment. Data shown are means ± SD of at least 16 cells per sample. Results shown are representative of more than three independent experiments. *$P < 0.01$.

(NAC) (Figure 3D and 3E). From the results of the present study, we suggest that ROS play an important role in cellular responses such as nSP-induced DNA damage. However, the reason why ROS generation varies with particle size has not yet been clarified.

Fine or ultrafine particulate matter (PM), such as diesel exhaust particles or crystalline silica, often induces ROS generation that contributes to the induction of DNA damage or apoptosis. Although the mechanisms underlying the PM-induced oxidative stress response remains unclear, strong evidence supports PM phagocytosis as a stimulus for increased oxidative stress *via* NADPH oxidase activation [38,42,43]. In addition, Walee Chamulitrat *et al.* reported that HaCaT cells constitutively express Nox components Rac1, p40phox, and p67phox proteins [44]. In HaCaT skin keratinocyte cells, stimuli such as epidermal growth factor, Ca^{2+}-ionophore A23187, lysophosphatidic acid are capable of producing ROS [45-47]. Thus, one potential candidate for the nSP70-mediated DNA damage is ROS, which is produced by NADPH oxidase upon nSP70 phagocytosis. In order to assess the relationship between the uptake pathway and ROS generation, we measured the production of ROS induced by nSP70 in the presence or absence of a specific inhibitor of endocytosis. After treatment with cytochalasin D, an inhibitor of actin polymerization [48], ROS generation induced by nSP70 was measured by DCFH-DA assay. Results indicated that ROS generation induced by nSP70 was inhibited by pretreatment with cytochalasin D in a dose-dependent manner (Figure 4). Furthermore, nSP70-induced DNA damage was also significantly reduced by pretreatment with cytochalasin D (Figure 5A and 5B). These findings suggest that the silica particles entered the cells mainly through actin-mediated endocytosis, such as the macropinocytosis pathway, thereby inducing ROS generation and DNA damage. It is well-known that NADPH oxidase, which exists in the cytosol, cellular membrane and subcellular compartment membranes, becomes activated and generates ROS after ingestion of microorganisms into the phagosome and/or endosome [49-51]. Moreover, it is reported that TiO_2 particles induce IL-1ß production by NADPH oxidase-mediated ROS generation in the human macrophage cell line [52]. Likewise, NADPH oxidase exists in the cytosol and membranes of non-phagocyte cells, including HaCaT cells [44]. Additionally, it had been reported that inflammasomes are activated by actin-mediated endocytosis of crystalline silica, which lead to NADPH oxidase activation and ROS generation [38,39,53]. Consequently, in order to determine the role of NADPH oxidase in silica particle-induced ROS generation, the effects of pretreatment with the NADPH oxidase inhibitor, apocynin, a well-known NOX inhibitor [49,54], were investigated. As

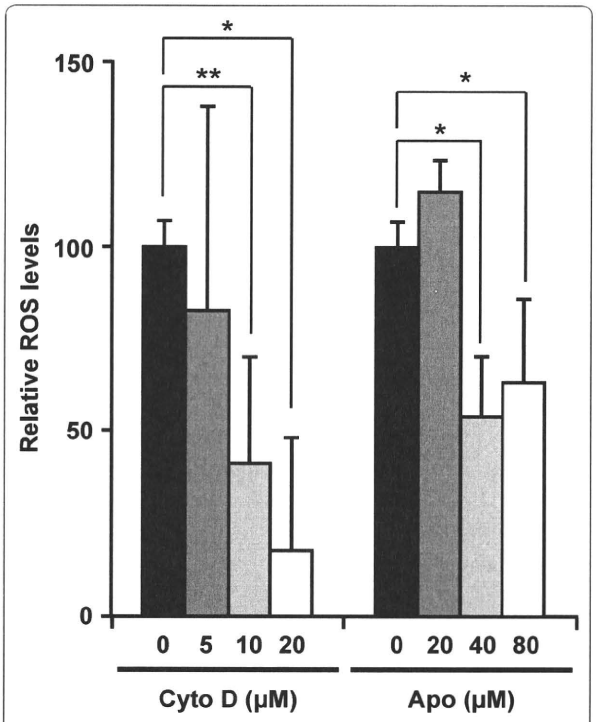

Figure 4 Effects of endocytosis and NADPH oxidase inhibitor on generation of ROS induced by silica particle treatment. HaCaT cells were pretreated with cytochalasin D or apocynin for 30 min prior to incubation with 270 mg/ml nSP70 for 3 h. ROS induced by silica particle treatment were expressed as relative fluorescence units, which means that ROS intensity of each silica particle alone and non-treatment is 100 and 0 respectively, in the DCFH assay. Data shown are means ± SD (n = 3). $^*P < 0.01$, $^{**}P < 0.05$.

expected, nSP70-induced ROS generation was inhibited in the presence of apocynin (Figure 4). In contrast, DNA damage induced by nSP70 was not inhibited by pretreatment with apocynin (Figure 5C and 5D). Taken together, these results suggest that nSP70-mediated DNA damage was induced by ROS generated by an unknown mechanism, and not *via* NADPH oxidase. Nox1 activation may initiate large bursts of ROS that can mediate the killing of pathogens, such as *H. pylori* [55]. Thus, NOX1 activation has been implicated in the cutaneous innate immunity to bacterial infections of the skin. A more detailed evaluation of the mechanism that underlies nSP70-mediated NOX activation is essential. Nonetheless, based on our results and the work of others, we speculate that nSP70s are treated almost like pathogens by HaCaT cells.

A number of mechanisms underlie the ability of nanoparticles to cause DNA damage. As mentioned above, a key mechanism that is often described is the ability of particles to cause the production of ROS [32,56]. One possible mechanism of particle-mediated DNA damage

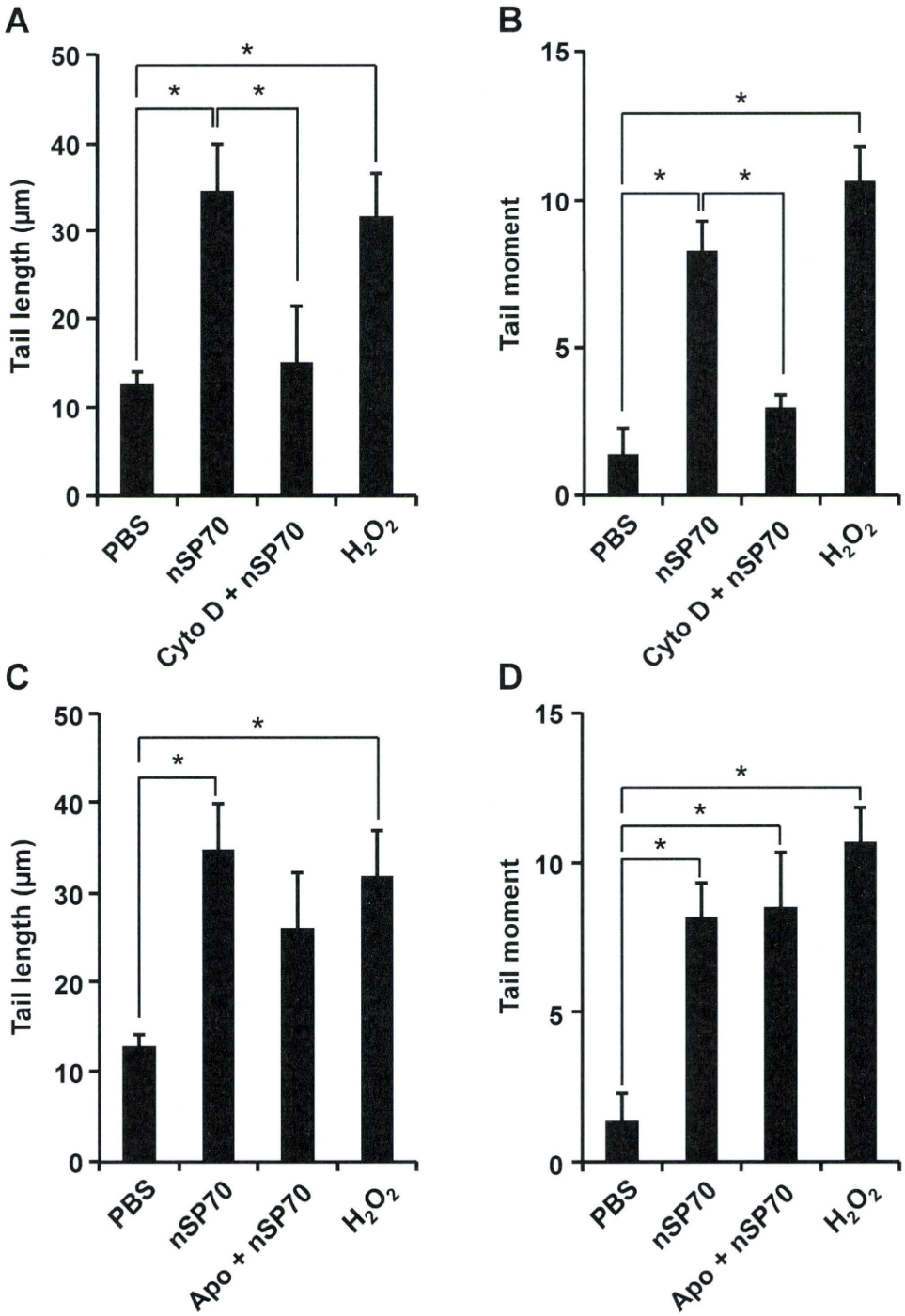

Figure 5 Effects of endocytosis and NADPH oxidase inhibitor on DNA damage by silica particle treatment. Effects of endocytosis inhibitor (**A and B**) or NADPH oxidase inhibitor (**C and D**) on DNA strand breaks induced by silica particle treatment in HaCaT cells. (**A and B**) HaCaT cells were pretreated with 10 mM cytochalasin D (Cyto D) for 30 min (Cyto D + nSP70) or nSP70 alone, prior to incubation with 90 mg/ml nSP70 for 3 h. (**C and D**) HaCaT cells were pretreated with 40 mM apocynin (Apo) for 30 min (Apo + nSP70) or nSP70 alone, prior to incubation with 90 mg/ml nSP70 for 3 h. As a positive control, HaCaT cells were treated with 0.2 mM H_2O_2 for 3 h. (**A and C**) Column height shows the tail length. (**B and D**) Column height shows the tail moment. Data shown are means ± SD of at least 16 cells per sample. Results shown are representative of more than three independent experiments. *$P < 0.01$.

is the ability of particles to stimulate target cells to produce oxidants/genotoxic compounds e.g., by affecting mitochondrial electron transport, activation of NADPH oxidase, or inducing cytochrome P450 enzymes. Our results show that nSP70-mediated DNA damage of HaCaT cells occurred *via* a mechanism that did not involve NADPH oxidase. Alternatively, transition metal ions (such as cadmium, chromium, cobalt, copper, iron, nickel, titanium and zinc) released from certain nanoparticles have the potential to cause the conversion of cellular oxygen metabolic products such as H_2O_2 and superoxide anions to hydroxyl radicals, which is one of the primary DNA damaging species. Well-known examples of the consequences of metal ion-contamination in relation to nanotoxicity have been described for carbon nanotubes. Indeed, iron contaminants in CNT have been shown to result in a substantial loss of glutathione and increased lipid peroxidation in alveolar macrophages, indicators of oxidative stress [57]. However, our data suggests that the nSPs used in this study, nSP70, nSP300 and mSP1000, were not contaminated with metal ions (data not shown). Thus, it is highly unlikely that metal ion contamination is involved in nSP70-induced DNA damage. Another hypothesis is that the size of nSPs is related to its oxidative stress. As particle size decreases, the particle unit of mass and overall surface area increases. This larger surface area enhances catalytic activity. Indeed, it has been widely reported that increased surface area of these particles increases reactivity because surface atoms have a tendency to possess high energy bonds. In order to gain stabilization, these surface bonds will readily react with other molecules [58]. The specific surface area was calculated by means of the following equation; $s = 6/d\rho$ (where s, specific surface area (m^2/g); ρ, density (g/cc); d, diameter (μm)). The specific surface area of nSP70, nSP300 and mSP1000 calculated using this equation was 43, 10 and 3 m^2/g, respectively. When specific area is considered, rather than particle concentration, the membrane damage activity of nSP70 and nSP300-treated cells shows almost the same level of LDH release per unit surface area (data not shown). In terms of ROS generation and DNA oxidation, nSP70 is more potent than nSP300. These results suggest that nSP70, which possesses a larger specific surface area compared to the counterpart micron-sized silica particles, has a much greater chance of interaction with biomolecules. Consequently, nSP70 causes direct cellular damage and promotion of oxidative stress. In addition to these hypotheses, nanoparticles may gain direct access to DNA *via* nuclear transport. However, this mechanism seems very unlikely given that the nuclear pore complex is known to be 8-30 nm in diameter, depending on cell type [59]. Nonetheless, some studies have reported that nanoparticles can penetrate the nuclear membrane, such as silica nanoparticles (40-70 nm) [60]. Detailed analysis of the mechanism of DNA damage induced by nanoparticles is currently underway. This information will be a critical determinant in the design of safer nSPs and will provide valuable information for hazard assessment of nSPs.

Here, we report the effects induced by well-dispersed amorphous silica particles (nSPs) on human keratinocyte (HaCaT) cells. In addition to our own work, other studies have shown that well-dispersed nSPs induce cytotoxicity, including LDH release, in a dose-dependent and size-dependent manner using a macrophage cell line [61,62]. On the other hands, Lin et al. reported that nSPs mediated cytotoxicity/DNA damage against A549 cells were not correlated with particle size [36]. Further, Barnes et al. reported that nSP induce no genotoxicity in fibroblast 3T3-L1 cells [63]. From the viewpoint of nSP-mediated toxicity, there is no consistency in these four reports including our findings. As mentioned above, there are a number of examples in the literature of conflicting results regarding nSPs. It has becoming increasingly evident that the physicochemical properties of nanomaterials, such as the size, shape, surface charge, fabricating method, etc, play a central role in governing their cellular uptake and subsequent physiologic consequences. Furthermore, experimental conditions, such as cell type and incubation time, are critical for the nanotoxicologic studies. Hence, given the inconsistencies it is difficult to draw the same conclusions. However, our results using well-dispersed nSPs indicated that nSPs were more cytotoxic and genotoxic against the human keratinocyte cell line HaCaT.

Conclusions

In this study, we show that nSP induce certain cellular responses, such as ROS generation and DNA damage. By contrast, their bulk-sized counterparts display a much reduced response. These different responses might be partly due to different mechanisms, such as intracellular uptake and ROS generation. We speculated that receptor-mediated uptake was involved in these phenomena and set out to identify the physicochemical properties that affect receptor endocytosis. We believe a detailed analysis of nSP-internalization will be invaluable for both hazard assessment and the design of safe nSPs.

Materials and methods

Silica particles

Suspensions of fluorescent (red-F)-labeled amorphous silica particles (Micromod Partikeltechnologie GmbH) (25 mg/ml and 50 mg/ml) were used in this study; particle size diameters were 70, 300 and 1000 nm (designated as nSP70, nSP300 and mSP1000,

respectively). Silica particle suspensions were stored in the dark at room temperature. The suspensions were sonicated for 5 min and then vortexed for 1 min immediately prior to use.

Cell Culture

The HaCaT human keratinocyte cell line was kindly provided by Dr. Inui [64], Osaka University. HaCaT cells were cultured in Dulbecco's modified Eagle's medium (D-MEM) supplemented with 10% heat-inactivated fetal bovine serum and 0.2 mM L-glutamine. The cells were grown in a humidified incubator at 37°C (95% room air, 5% CO_2).

Physicochemical examinations of silica particles

Silica particle suspensions were diluted to 0.25 mg/ml (nSP70), 0.5 mg/ml (nSP300 and mSP1000) with water or PBS, respectively and the average particle sizes were then measured using the Zetasizer Nano-ZS (Malvern Instruments Ltd). The mean size and the size distribution of silica particles were measured by a dynamic light scattering method. The size and shape of silica particles were determined using scanning electron microscopy (SEM). Each silica particle suspension was dropped on the sample stage and dried. The dried silica particles were then observed by SEM.

LDH release assay

Lactate dehydrogenase (LDH) is released from HaCaT cells exposed to nSP70, nSP300 or mSP1000. The LDH activity of the supernatant of the culture medium was determined using a commercial LDH cytotoxicity test (WAKO, Japan) according to the manufacturer's instructions. In brief, 5×10^3 cells were seeded into each well of a 96-well plate. After 24 h incubation, cells were treated with nSP70, nSP300, mSP1000 or 0.2% Tween 20 (positive control). After a further 24 h incubation period, 50 μl of medium overlying cells was used for LDH analysis. Absorption of light at 560 nm was measured using a spectrophotometer.

Detection of Reactive Oxygen Species (ROS)

The generation of total intracellular ROS was measured by monitoring the increasing fluorescence of 2'7'-dichlorofluorescein (DCF). The cell-permeant 2'7'-dichlorodihydorofluorescein diacetate (DCFH-DA; Sigma, St. Louis, MO) enters the cell where intracellular esterases cleave off the diacetate group. The resulting DCFH is retained in the cytoplasm and oxidized to DCF by ROS. Hydroxyl radical was measured by monitoring the increasing fluorescence of hydroxyphenyl fluorescein (HPF; SEKISUI MEDICAL Co., Ltd., Japan). 3×10^4 HaCaT cells were seeded into each well of a 96-well plate. After 24 h incubation, cells were treated with nSP70, nSP100, nSP300, mSP1000 or 2 mM H_2O_2 (positive control). Cells were then washed once with phenol red-free medium, and incubated in 100 μl working solution of DCFH-DA or HPF (10 μM) at 37°C for 30 min. Using the fluorescence reader (ARVO MX; Perkin Elmer, Waltham, MA), the fluorescence of DCF or HPF was monitored at the excitation and emission wavelengths of 485 nm and 530 nm or 490 nm and 515 nm, respectively.

8-Hydroxy-2-deoxyguanosine (8-OH-dG) measurement

HaCaT cells were seeded on a 100 mm dish. After 24 h, cells were treated with various concentrations of nSP70, nSP300, mSP1000, 0.2 mM H_2O_2 (positive control) or PBS (negative control). After 3 h, cellular DNA was isolated using DNeasy tissue kit (QIAGEN, Germany). Ten μg of DNA was converted to single stranded DNA by incubation with 180 U Exonuclease III (Takara Biotech., Japan) at 37°C for 1 h. The DNA was heated at 95°C for 5 min, rapidly chilled on ice, and digested to nucleosides by incubation with 0.6 U nuclease P1 (Takara) at 37°C for 1 h followed by treatment with 0.6 U *E. coli* alkaline phosphatase (Takara) for a further 1 h. The reaction mixture was centrifuged (6000 × g for 1 min) and the supernatant used for the 8-OHdG assay. The amount of 8-OHdG was measured according to the protocol of the competitive ELISA kit (8-OHdG check; Japan Institute for the Control of Aging, Japan).

Effects of inhibitor of ROS, endocytosis or NADPH oxidase on DNA strand breaks induced by silica particles

3×10^4 HaCaT cells were pretreated with 2 mM N-acetylcystein (NAC, ROS scavenger), 10 mM cytochalasin D (endocytosis inhibitor) or 40 mM apocynin (NADPH oxidase inhibitor) for 30 min prior to incubation with 90 mg/ml of nSP70 for 3 h. As a positive control, HaCaT cells were treated with 0.2 mM H_2O_2 for 3 h. DNA strand breaks were detected by alkaline comet assay according to the Comet Assay Kit (Trevigen, Gaithersburg, MD). The samples were processed according to the protocol provided in the kit. Twenty-five cells on each slide, randomly selected by fluorescence microscopy, were then analyzed using the Comet Analyzer (Youworks Corporation, Japan).

Effects of inhibitor of endocytosis, NADPH oxidase or endosomal acidification on generation of ROS induced by silica particles

HaCaT cells were pretreated with various concentration of cytochalasin D (Merck Ltd., Germany) for 30 min prior to incubation with 270 mg/ml nSP70 for 3 h. ROS induced by treatment with silica particles were expressed as relative fluorescence units in the DCFH-DA assay as described above.

Statistical analysis

Statistical comparisons between groups were performed by one-way ANOVA and a Bonferroni *post hoc* test. The level of significance was set at $P < 0.05$.

Acknowledgements

This study was supported in part by Grants-in-Aid for Scientific Research from the Ministry of Education, Culture, Sports, Science and Technology of Japan, and from the Japan Society for the Promotion of Science (JSPS). This study was also supported in part by Health Labour Sciences Research Grants from the Ministry of Health, Labor and Welfare of Japan; by Health Sciences Research Grants for Research on Publicly Essential Drugs and Medical Devices from the Japan Health Sciences Foundation; by a Global Environment Research Fund from Minister of the Environment; and by a the Knowledge Cluster Initiative; and by Food Safety Commission; and by The Nagai Foundation Tokyo; and by The Cosmetology Research Foundation; and by The Smoking Research Foundation.

Author details

[1]Graduate School of Pharmaceutical Sciences, Osaka University, 1-6 Yamadaoka, Suita, Osaka 565-0871, Japan. [2]Laboratory of Biopharamceutical Research (Pharmaceutical Proteomics), National Institute of Biomedical Innovation, 7-6-8, Saito-Asagi, Ibaraki, Osaka, 567-0085, Japan. [3]The Center for Advanced Medical Engineering and Informatics, Osaka University, 1-6, Yamadaoka, Suita, Osaka, 565-0871, Japan.

Authors' contributions

HN and TY designed the study. HN, KM, YN, STo, SK, TH and TA performed experiments. HN and TY collected and analysed data. HN and TY wrote the manuscript. KN, YA, YY, HK, NI and STs gave technical support and conceptual advice. YT supervised the all of projects. All authors discussed the results and commented on the manuscript.

Competing interests

The authors declare that they have no competing interests.

Received: 13 September 2010 **Accepted:** 15 January 2011
Published: 15 January 2011

References

1. Salata O: **Applications of nanoparticles in biology and medicine.** *J Nanobiotechnology* 2004, **2**:3.
2. Aiso S, Yamazaki K, Umeda Y, Asakura M, Takaya M, Toya T, Koda S, Nagano K, Arito H, Fukushima S: **Pulmonary Toxicity of Intratracheally Instilled Multiwall Carbon Nanotubes in Male Fischer 344 Rats.** *Ind Health* 2010.
3. Chen J, Dong X, Zhao J, Tang G: **In vivo acute toxicity of titanium dioxide nanoparticles to mice after intraperitioneal injection.** *J Appl Toxicol* 2009, **29**:330-337.
4. Geys J, Nemmar A, Verbeken E, Smolders E, Ratoi M, Hoylaerts MF, Nemery B, Hoet PH: **Acute toxicity and prothrombotic effects of quantum dots: impact of surface charge.** *Environ Health Perspect* 2008, **116**:1607-1613.
5. Heng BC, Zhao X, Xiong S, Ng KW, Boey FY, Loo JS: **Toxicity of zinc oxide (ZnO) nanoparticles on human bronchial epithelial cells (BEAS-2B) is accentuated by oxidative stress.** *Food Chem Toxicol* 2010, **48**:1762-1766.
6. Kocbek P, Teskac K, Kreft ME, Kristl J: **Toxicological Aspects of Long-Term Treatment of Keratinocytes with ZnO and TiO(2) Nanoparticles.** *Small* 2010, **6**:1908-1917.
7. Liu S, Xu L, Zhang T, Ren G, Yang Z: **Oxidative stress and apoptosis induced by nanosized titanium dioxide in PC12 cells.** *Toxicology* 2010, **267**:172-177.
8. Moos PJ, Chung K, Woessner D, Honeggar M, Cutler NS, Veranth JM: **ZnO particulate matter requires cell contact for toxicity in human colon cancer cells.** *Chem Res Toxicol* 2010, **23**:733-739.
9. Murray AR, Kisin E, Leonard SS, Young SH, Kommineni C, Kagan VE, Castranova V, Shvedova AA: **Oxidative stress and inflammatory response in dermal toxicity of single-walled carbon nanotubes.** *Toxicology* 2009, **257**:161-171.
10. Park EJ, Kim H, Kim Y, Yi J, Choi K, Park K: **Carbon fullerenes (C60s) can induce inflammatory responses in the lung of mice.** *Toxicol Appl Pharmacol* 2010, **244**:226-233.
11. Poland CA, Duffin R, Kinloch I, Maynard A, Wallace WA, Seaton A, Stone V, Brown S, Macnee W, Donaldson K: **Carbon nanotubes introduced into the abdominal cavity of mice show asbestos-like pathogenicity in a pilot study.** *Nat Nanotechnol* 2008, **3**:423-428.
12. Shin JA, Lee EJ, Seo SM, Kim HS, Kang JL, Park EM: **Nanosized titanium dioxide enhanced inflammatory responses in the septic brain of mouse.** *Neuroscience* 2010, **165**:445-454.
13. Takagi A, Hirose A, Nishimura T, Fukumori N, Ogata A, Ohashi N, Kitajima S, Kanno J: **Induction of mesothelioma in p53+/- mouse by intraperitoneal application of multi-wall carbon nanotube.** *J Toxicol Sci* 2008, **33**:105-116.
14. Yamashita K, Yoshioka Y, Higashisaka K, Morishita Y, Yoshida T, Fujimura M, Kayamuro H, Nabeshi H, Yamashita T, Nagano K, *et al*: **Carbon nanotubes elicit DNA damage and inflammatory response relative to their size and shape.** *Inflammation* 2010, **33**:276-280.
15. Chen Z, Meng H, Xing G, Chen C, Zhao Y, Jia G, Wang T, Yuan H, Ye C, Zhao F, *et al*: **Acute toxicological effects of copper nanoparticles in vivo.** *Toxicol Lett* 2006, **163**:109-120.
16. Duan Y, Liu J, Ma L, Li N, Liu H, Wang J, Zheng L, Liu C, Wang X, Zhao X, *et al*: **Toxicological characteristics of nanoparticulate anatase titanium dioxide in mice.** *Biomaterials* 2010, **31**:894-899.
17. Li JJ, Muralikrishnan S, Ng CT, Yung LY, Bay BH: **Nanoparticle-induced pulmonary toxicity.** *Exp Biol Med (Maywood)* 2010, **235**:1025-1033.
18. Li N, Duan Y, Hong M, Zheng L, Fei M, Zhao X, Wang J, Cui Y, Liu H, Cai J, *et al*: **Spleen injury and apoptotic pathway in mice caused by titanium dioxide nanoparticules.** *Toxicol Lett* 2010, **195**:161-168.
19. Liang G, Yin L, Zhang J, Liu R, Zhang T, Ye B, Pu Y: **Effects of subchronic exposure to multi-walled carbon nanotubes on mice.** *J Toxicol Environ Health A* 2010, **73**:463-470.
20. Sung JH, Ji JH, Yoon JU, Kim DS, Song MY, Jeong J, Han BS, Han JH, Chung YH, Kim J, *et al*: **Lung function changes in Sprague-Dawley rats after prolonged inhalation exposure to silver nanoparticles.** *Inhal Toxicol* 2008, **20**:567-574.
21. Nishimori H, Kondoh M, Isoda K, Tsunoda S, Tsutsumi Y, Yagi K: **Silica nanoparticles as hepatotoxicants.** *Eur J Pharm Biopharm* 2009, **72**:496-501.
22. Aillon KL, Xie Y, El-Gendy N, Berkland CJ, Forrest ML: **Effects of nanomaterial physicochemical properties on in vivo toxicity.** *Adv Drug Deliv Rev* 2009, **61**:457-466.
23. Hoshino A, Fujioka K, Oku T, Suga M, Sasaki FY, Ohta T, Yasuhara M, Suzuki K, Yamamoto K: **Physicochemical Properties and Cellular Toxicity of Nanocrystal Quantum Dots Depend on Their Surface Modification.** *Nano Letters* 2004, **4**:2163-2169.
24. Morishige T, Yoshioka Y, Inakura H, Tanabe A, Yao X, Narimatsu S, Monobe Y, Imazawa T, Tsunoda S, Tsutsumi Y, *et al*: **The effect of surface modification of amorphous silica particles on NLRP3 inflammasome mediated IL-1beta production, ROS production and endosomal rupture.** *Biomaterials* 2010, **31**:6833-6842.
25. Sohaebuddin SK, Thevenot PT, Baker D, Eaton JW, Tang L: **Nanomaterial cytotoxicity is composition, size, and cell type dependent.** *Part Fibre Toxicol* 2010, **7**:22.
26. Fourches D, Pu D, Tassa C, Weissleder R, Shaw SY, Mumper RJ, Tropsha A: **Quantitative nanostructure-activity relationship modeling.** *ACS Nano* 2010, **4**:5703-5712.
27. Puzyn T, Leszczynska D, Leszczynski J: **Toward the development of "nano-QSARs": advances and challenges.** *Small* 2009, **5**:2494-2509.
28. Shaw SY, Westly EC, Pittet MJ, Subramanian A, Schreiber SL, Weissleder R: **Perturbational profiling of nanomaterial biologic activity.** *Proc Natl Acad Sci USA* 2008, **105**:7387-7392.
29. Tropsha A, Golbraikh A: **Predictive QSAR modeling workflow, model applicability domains, and virtual screening.** *Curr Pharm Des* 2007, **13**:3494-3504.
30. Weissleder R, Kelly K, Sun EY, Shtatland T, Josephson L: **Cell-specific targeting of nanoparticles by multivalent attachment of small molecules.** *Nat Biotechnol* 2005, **23**:1418-1423.
31. Borm P, Klaessig FC, Landry TD, Moudgil B, Pauluhn J, Thomas K, Trottier R, Wood S: **Research strategies for safety evaluation of nanomaterials, part V: role of dissolution in biological fate and effects of nanoscale particles.** *Toxicol Sci* 2006, **90**:23-32.

32. Nel A, Xia T, Madler L, Li N: **Toxic potential of materials at the nanolevel.** *Science* 2006, **311**:622-627.
33. Rahman IA, Vejayakumaran P, Sipaut SC, Ismail J, Chee KC: **Size-dependent physicochemical and optical properties of silica nanoparticles.** *Materials Chemistry and Physics* 2009, **114**:328-332.
34. Xia T, Kovochich M, Brant J, Hotze M, Sempf J, Oberley T, Sioutas C, Yeh JI, Wiesner MR, Nel AE: **Comparison of the abilities of ambient and manufactured nanoparticles to induce cellular toxicity according to an oxidative stress paradigm.** *Nano Lett* 2006, **6**:1794-1807.
35. Eom HJ, Choi J: **Oxidative stress of silica nanoparticles in human bronchial epithelial cell, Beas-2B.** *Toxicol In Vitro* 2009, **23**:1326-1332.
36. Lin W, Huang YW, Zhou XD, Ma Y: **In vitro toxicity of silica nanoparticles in human lung cancer cells.** *Toxicol Appl Pharmacol* 2006, **217**:252-259.
37. Wang F, Gao F, Lan M, Yuan H, Huang Y, Liu J: **Oxidative stress contributes to silica nanoparticle-induced cytotoxicity in human embryonic kidney cells.** *Toxicol In Vitro* 2009, **23**:808-815.
38. Dostert C, Petrilli V, Van Bruggen R, Steele C, Mossman BT, Tschopp J: **Innate immune activation through Nalp3 inflammasome sensing of asbestos and silica.** *Science* 2008, **320**:674-677.
39. Hornung V, Bauernfeind F, Halle A, Samstad EO, Kono H, Rock KL, Fitzgerald KA, Latz E: **Silica crystals and aluminum salts activate the NALP3 inflammasome through phagosomal destabilization.** *Nat Immunol* 2008, **9**:847-856.
40. Ames BN: **Dietary carcinogens and anticarcinogens. Oxygen radicals and degenerative diseases.** *Science* 1983, **221**:1256-1264.
41. Harman D: **The aging process.** *Proc Natl Acad Sci USA* 1981, **78**:7124-7128.
42. Li Z, Hyseni X, Carter JD, Soukup JM, Dailey LA, Huang YC: **Pollutant particles enhanced H2O2 production from NAD(P)H oxidase and mitochondria in human pulmonary artery endothelial cells.** *Am J Physiol Cell Physiol* 2006, **291**:C357-365.
43. Wang T, Chiang ET, Moreno-Vinasco L, Lang GD, Pendyala S, Samet JM, Geyh AS, Breysse PN, Chillrud SN, Natarajan V, Garcia JG: **Particulate matter disrupts human lung endothelial barrier integrity via ROS- and p38 MAPK-dependent pathways.** *Am J Respir Cell Mol Biol* 2010, **42**:442-449.
44. Chamulitrat W, Stremmel W, Kawahara T, Rokutan K, Fujii H, Wingler K, Schmidt HH, Schmidt R: **A constitutive NADPH oxidase-like system containing gp91phox homologs in human keratinocytes.** *J Invest Dermatol* 2004, **122**:1000-1009.
45. Goldman R, Moshonov S, Zor U: **Generation of reactive oxygen species in a human keratinocyte cell line: role of calcium.** *Arch Biochem Biophys* 1998, **350**:10-18.
46. Goldman R, Moshonov S, Zor U: **Calcium-dependent PAF-stimulated generation of reactive oxygen species in a human keratinocyte cell line.** *Biochim Biophys Acta* 1999, **1438**:349-358.
47. Sekharam M, Cunnick JM, Wu J: **Involvement of lipoxygenase in lysophosphatidic acid-stimulated hydrogen peroxide release in human HaCaT keratinocytes.** *Biochem J* 2000, **346(Pt 3)**:751-758.
48. Sampath P, Pollard TD: **Effects of cytochalasin, phalloidin, and pH on the elongation of actin filaments.** *Biochemistry* 1991, **30**:1973-1980.
49. Lambeth JD: **NOX enzymes and the biology of reactive oxygen.** *Nat Rev Immunol* 2004, **4**:181-189.
50. Li Q, Zhang Y, Marden JJ, Banfi B, Engelhardt JF: **Endosomal NADPH oxidase regulates c-Src activation following hypoxia/reoxygenation injury.** *Biochem J* 2008, **411**:531-541.
51. Ushio-Fukai M: **Localizing NADPH oxidase-derived ROS.** *Sci STKE* 2006, **2006**:re8.
52. Morishige T, Yoshioka Y, Tanabe A, Yao X, Tsunoda S, Tsutsumi Y, Mukai Y, Okada N, Nakagawa S: **Titanium dioxide induces different levels of IL-1beta production dependent on its particle characteristics through caspase-1 activation mediated by reactive oxygen species and cathepsin B.** *Biochem Biophys Res Commun* 2010, **392**:160-165.
53. Fubini B, Hubbard A: **Reactive oxygen species (ROS) and reactive nitrogen species (RNS) generation by silica in inflammation and fibrosis.** *Free Radic Biol Med* 2003, **34**:1507-1516.
54. Meyer JW, Schmitt ME: **A central role for the endothelial NADPH oxidase in atherosclerosis.** *FEBS Lett* 2000, **472**:1-4.
55. Kawahara T, Kuwano Y, Teshima-Kondo S, Kawai T, Nikawa T, Kishi K, Rokutan K: **Toll-like receptor 4 regulates gastric pit cell responses to Helicobacter pylori infection.** *J Med Invest* 2001, **48**:190-197.
56. Schins RP: **Mechanisms of genotoxicity of particles and fibers.** *Inhal Toxicol* 2002, **14**:57-78.
57. Kagan VE, Tyurina YY, Tyurin VA, Konduru NV, Potapovich AI, Osipov AN, Kisin ER, Schwegler-Berry D, Mercer R, Castranova V, Shvedova AA: **Direct and indirect effects of single walled carbon nanotubes on RAW 264.7 macrophages: role of iron.** *Toxicol Lett* 2006, **165**:88-100.
58. Oberdorster G, Geleinr R, Johnston C, Mercer P, Corson N, Finkelstein J: **Ambient ultra fine particles: Inducers of acute Lung injury? Relationships between respiratory disease and exposure to air pollution.** ILSI Press, Washington, DC; 1998, 216-229.
59. Terry LJ, Shows EB, Wente SR: **Crossing the nuclear envelope: hierarchical regulation of nucleocytoplasmic transport.** *Science* 2007, **318**:1412-1416.
60. Chen M, von Mikecz A: **Formation of nucleoplasmic protein aggregates impairs nuclear function in response to SiO2 nanoparticles.** *Exp Cell Res* 2005, **305**:51-62.
61. Lison D, Thomassen LC, Rabolli V, Gonzalez L, Napierska D, Seo JW, Kirsch-Volders M, Hoet P, Kirschhock CE, Martens JA: **Nominal and effective dosimetry of silica nanoparticles in cytotoxicity assays.** *Toxicol Sci* 2008, **104**:155-162.
62. Waters KM, Masiello LM, Zangar RC, Tarasevich BJ, Karin NJ, Quesenberry RD, Bandyopadhyay S, Teeguarden JG, Pounds JG, Thrall BD: **Macrophage responses to silica nanoparticles are highly conserved across particle sizes.** *Toxicol Sci* 2009, **107**:553-569.
63. Barnes CA, Elsaesser A, Arkusz J, Smok A, Palus J, Lesniak A, Salvati A, Hanrahan JP, Jong WH, Dziubaltowska E, *et al*: **Reproducible comet assay of amorphous silica nanoparticles detects no genotoxicity.** *Nano Lett* 2008, **8**:3069-3074.
64. Inui S, Lee YF, Haake AR, Goldsmith LA, Chang C: **Induction of TR4 orphan receptor by retinoic acid in human HaCaT keratinocytes.** *J Invest Dermatol* 1999, **112**:426-431.

doi:10.1186/1743-8977-8-1
Cite this article as: Nabeshi *et al.*: Amorphous nanosilica induce endocytosis-dependent ROS generation and DNA damage in human keratinocytes. *Particle and Fibre Toxicology* 2011 **8**:1.

synthesis[6,7]. Improved rate capabilities and the potential for integrated three-dimensional batteries to provide enough energy to microdevices, even when space is limited, have been pointed out in the earlier investigations[4–6]. Bicontinuous electrode structures that combine electrolytically active and conductive phases, too, have been investigated[8–10]. However, the particular combination developed in the paper by Braun and co-workers leads to significantly better rate capabilities owing to the highly conductive metal backbone. Thus they represent an exemplary combination of the high power densities of supercapacitors with the high energy densities of batteries. Furthermore, the approach of combining an active electrode material with a conductive scaffold may allow the use of high-capacity electrode materials that had been previously ignored because of low conductivities.

There are other opportunities for improving performance. In the present design, the nickel scaffold contributes to the mass of the electrode but not to its capacity. Conducting scaffolds with lower mass densities would improve the capacity of the electrode per unit mass. Similarly, less open-pore space would improve the capacity per unit volume, as long as sufficient room for electrolyte penetration is still maintained. It is also possible to exploit the pore volume by threading the second battery electrode through it, forming a completely interpenetrating battery structure. Although this is challenging from a processing perspective, the synthetic feasibility of this concept has already been demonstrated[7], and such an approach may eventually be adapted to fabricate all solid-state, high-performance batteries.

Another challenge for these electrode designs is heat management, which will be important given the large currents per unit mass they must support. Nonetheless, the work by Braun and co-workers[1] represents an elegant and important step forward in the development of new electrochemical storage devices. It clearly shows that considerations of electrode architecture and electrode composition must go hand-in-hand to push performance limits forward. ❐

Andreas Stein is in the Department of Chemistry, University of Minnesota, Minneapolis, Minnesota 55455, USA.
e-mail: a-stein@umn.edu

References

1. Zhang, H., Yu, X. & Braun, P. V. *Nature Nanotech.* **6,** 277–281 (2011).
2. Tetreault, N., Miguez, H. & Ozin, G. A. *Adv. Mater.* **16,** 1471–1476 (2004).
3. Bruce, P. G., Scrosati, B. & Terascon, J. M. *Angew. Chem. Int. Ed.* **47,** 2930–2946 (2008).
4. Sakamoto, J. S. & Dunn, B. *J. Mater. Chem.* **12,** 2859–2861 (2002).
5. Lee, K. T., Lytle, J. C., Ergang, N. S., Oh, S. M. & Stein, A. *Adv. Funct. Mater.* **15,** 547–556 (2005).
6. Long, J. W., Dunn, B., Rolison, D. R. & White, H. S. *Chem. Rev.* **104,** 4463–4492 (2004).
7. Ergang, N. S. *et al. Adv. Mater.* **18,** 1750–1753 (2006).
8. Fischer, A. E., Pettigrew, K. A., Rolison, D. R., Stroud, R. M. & Long, J. W. *Nano Lett.* **7,** 281–286 (2007).
9. Ji, X., Lee, K. T. & Nazar, L. F. *Nature Mater.* **8,** 500–506, (2009).
10. Doherty, C. M., Caruso, R. A., Smarsly, B. M., Adelhelm, P. & Drummond, C. J. *Chem. Mater.* **21,** 5300–5306 (2009).

NANOTOXICOLOGY

Nanoparticles versus the placenta

Pregnant mice treated 70-nm silica nanoparticles or 35-nm titanium dioxide nanoparticles suffer damage to the placenta and fetus, whereas larger nanoparticles do not have an adverse impact.

Jeffrey A. Keelan

As the likelihood of humans being exposed to nanomaterials increases, there are growing concerns about the effects of nanoparticles on pregnant women[1,2] and the possibility that they can cross the placenta and cause toxicity in the fetus[3–6]. Now, writing in *Nature Nanotechnology*, Kohei Yamashita, Yasuo Yoshioka, Yasuo Tsutsumi and colleagues confirm that some nanoparticles can cross the placenta and accumulate in fetuses in pregnant mice[7]. Moreover, they also show that nanoparticles can restrict the growth of the fetus through damage to the placenta, although these effects could be prevented by changing their surface charge.

The mouse (or murine) placenta is like the human placenta in that the maternal and fetal blood supplies are separated by the endothelium and one or more layers of specialized placental cells called trophoblasts (Fig. 1)[7]. However, there are also significant differences: the number of cellular layers and the diffusion distance between the two circulations both differ, and the diffusion barrier in the murine placenta is significantly greater than in the human placenta. Pregnant mice also have a large inverted yolk sac that performs important functions throughout pregnancy, whereas the yolk sac is less important in humans except during early pregnancy. Consequently, although the mouse model is very useful for research, care must be taken when extrapolating the results to human pregnancy.

Yamashita and co-workers — who are based at Osaka University, the National Institute of Biomedical Innovation and other institutes in Japan — exposed pregnant mice to silica nanoparticles with three different diameters (70, 300 and 900 nm) on day 16 of pregnancy (~80% term). Silica nanoparticles are known to be able to enter cells, cause programmed cell death (apoptosis) and initiate a systemic immune response. As expected, most of the nanoparticles accumulated in the maternal liver. The 70-nm nanoparticles were also found in the placenta and were detectable in the fetal liver and brain, proving that they had breached the placental barrier and entered the fetal circulation. However, the 300- and 900-nm nanoparticles did not accumulate in the placenta or reach the fetus. The motivation for such experiments is to explore the potential toxicity of nanoparticles from all sources to pregnant women, and also to investigate the safety of nanoparticles introduced into the body for medical applications during pregnancy.

The results of the Japanese group are consistent with findings from *ex vivo* perfusion studies using human placentas, which suggested that size is an important determinant of placental uptake, with particles larger than ~80 nm being partially or totally excluded[8,9]. In the latest study, just two days of exposure to high doses of the 70-nm nanoparticles was enough to lead to significant placental damage (notably major abnormalities in placental structure and blood flow, plus reduced amniotic-sac size), fetal growth restriction and, in some cases, death of the fetus. The placental damage was accompanied by reduced levels of placental growth factors in the maternal circulation,

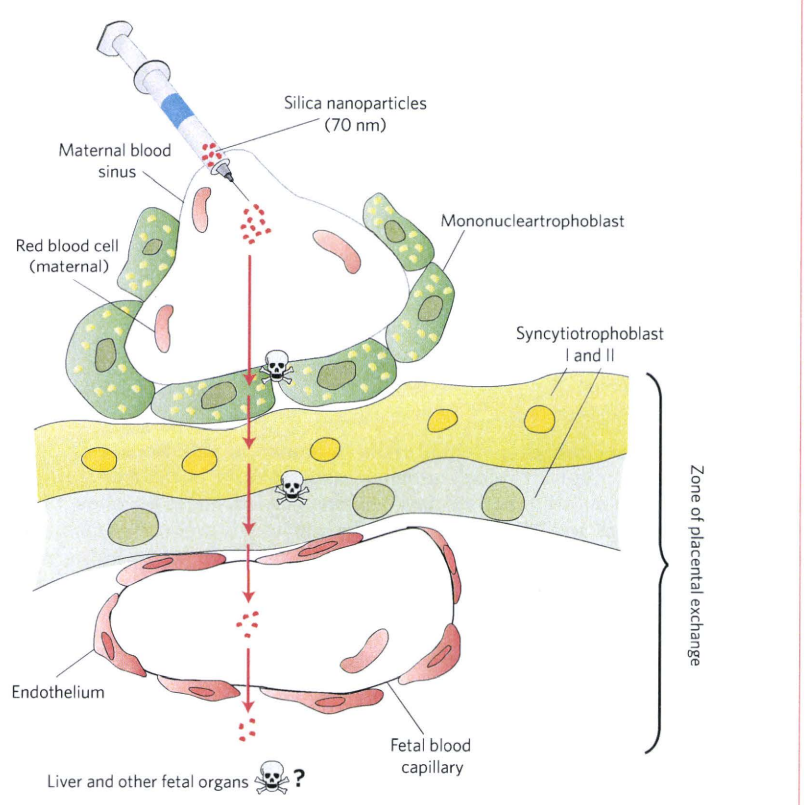

Figure 1 | Nanoparticles (shown in red) injected into the maternal blood supply (top) must pass through three layers of trophoblast cells to enter the fetal blood. Toxicity can occur at various stages of this process (indicated by the skull and cross bones). Yamashita and co-workers found that 70-nm nanoparticles caused damage to the placenta and disrupted fetal growth[7]. It is not yet clear if the disruption to fetal growth was caused by direct exposure to the nanoparticles, or by the damage to the placenta (hence the question mark beside the bottom skull and cross bones). Large nanoparticles and those coated with amine and carboxyl groups were not toxic.

which is evidence of both functional and structural impairment.

So how did the silica nanoparticles penetrate the placental barrier, and why were the 70-nm nanoparticles toxic when the 300- and 900-nm nanoparticles were not? It should be appreciated that the placenta is not actually a complete and effective barrier. Small molecules can readily diffuse through the placental tissues, whereas larger molecules can be taken up by endocytosis (in which objects are engulfed by the cell membrane); the yolk sac is particularly active in this regard. Perfusion studies on humans suggest that an endocytotic mechanism is probably responsible for allowing nanoparticle entry into the outer trophoblast layer of the placenta[9]. Although the murine yolk sac could contribute to this phenomenon, the fact that the nanoparticles were observed inside placental tissues suggests that placental transport is also significant, and the findings are likely to be pertinent to human pregnancy.

There is some evidence that silica nanoparticles enter the nucleus of cells and trigger apoptosis through their interaction with DNA. This may well be the mechanism responsible for the placental damage observed by Yamashita and co-workers. It is likely that there was also cell death in fetal organs (particularly the brain), although this was not explicitly investigated.

Similar effects were also caused by 35-nm titanium dioxide nanoparticles, which are also known to induce apoptosis after entering cells. If this is the mode of toxicity, it is notable that the Japanese team found that the deleterious effects of the nanoparticles could be reversed by coating the surface with carboxyl or amino groups. Other groups have recently shown that such modified nanoparticles are much less toxic than 'naked' nanoparticles owing to their inability to penetrate the nucleus (and therefore cause apoptosis), despite their ability to enter the cellular cytoplasm[10]. Unfortunately, cellular entry and apoptosis of the modified nanoparticles were not investigated in the present study.

These findings highlight the potential fetotoxicity of nanoparticle exposure in pregnancy, in particular the susceptibility of the placenta to circulating nanotoxins. They show that extreme caution is required when considering exposure of pregnant women to nanomaterials. However, the study also raises a number of important questions that have yet to be answered.

First, it is not known whether the size-dependent effects observed (that is, the placental transfer and fetoplacental toxicity) reflect an inherent size-exclusion property of the placenta itself, or a characteristic of the specific nanomaterials investigated in this study. If it is the former, then it opens the door to the design and use of therapeutic nanoparticles in pregnancy by adjusting the size to achieve either placental exclusion or placental uptake, depending on what is required[2]. Second, the relationship between fetal exposure to nanomaterials and toxicity needs to be clarified, as it is unknown whether the fetus can be exposed to non-cytotoxic nanomaterials without developmental defects and cellular damage; dose-dependency is another unresolved issue. Third, and finally, the mechanisms responsible for determining whether nanoparticles are transported from within the trophoblast layer into the fetal circulation are still unclear, as is the impact of nanoparticle size and surface properties on the degree of transport.

Answering these questions will help clarify the relationship between nanoparticle size, composition and fetoplacental toxicity, and give valuable guidance on the safety of nanomaterial exposure during pregnancy. ❐

Jeffrey Keelan is in the School of Women's and Infants' Health, University of Western Australia at King Edward Memorial Hospital, Subiaco, Perth, Western Australia 6009, Australia.
e-mail: jeff.keelan@uwa.edu.au

References

1. Saunders, M. *WIREs Nanomed. Nanobiotechnol.* **1,** 671–684 (2009).
2. Menezes, A., Malek, A. & Keelan, J. A. *Curr. Pharm. Biotechnol.* http://www.ncbi.nlm.nih.gov/pubmed/21342124 (2011).
3. Tsuchiya, T. *et al. FEBS Lett.* **393,** 139–145 (1996).
4. Fujimoto, A. *et al. Environ. Toxicol.* **20,** 431–440 (2005).
5. Takeda, K. *et al. J. Health Sci.* **55,** 95–102 (2009).
6. Semmler-Behnke, M. *et al. Small* **4,** 2108–2111 (2008).
7. Yamashita, K. *et al. Nature Nanotech.* **6,** 321–328 (2011).
8. Myllynen, P. K. *et al. Reprod. Toxicol.* **26,** 130–137 (2008).
9. Wick, P. *et al. Environ. Health Perspect.* **118,** 432–436 (2010).
10. Nabeshi, H. *et al. Nanoscale Res. Lett.* **6,** 93–98 (2011).

nature nanotechnology

ARTICLES

PUBLISHED ONLINE: 3 APRIL 2011 | DOI: 10.1038/NNANO.2011.41

Silica and titanium dioxide nanoparticles cause pregnancy complications in mice

Kohei Yamashita[1,2†], Yasuo Yoshioka[1,2,3†*], Kazuma Higashisaka[1,2], Kazuya Mimura[4], Yuki Morishita[1,2], Masatoshi Nozaki[4], Tokuyuki Yoshida[1,2], Toshinobu Ogura[1,2], Hiromi Nabeshi[1,2], Kazuya Nagano[2], Yasuhiro Abe[2], Haruhiko Kamada[2,3], Youko Monobe[5], Takayoshi Imazawa[5], Hisae Aoshima[6], Kiyoshi Shishido[7], Yuichi Kawai[8], Tadanori Mayumi[8], Shin-ichi Tsunoda[2,3,9], Norio Itoh[1], Tomoaki Yoshikawa[1,2], Itaru Yanagihara[4], Shigeru Saito[10] and Yasuo Tsutsumi[1,2,3*]

The increasing use of nanomaterials has raised concerns about their potential risks to human health. Recent studies have shown that nanoparticles can cross the placenta barrier in pregnant mice and cause neurotoxicity in their offspring, but a more detailed understanding of the effects of nanoparticles on pregnant animals remains elusive. Here, we show that silica and titanium dioxide nanoparticles with diameters of 70 nm and 35 nm, respectively, can cause pregnancy complications when injected intravenously into pregnant mice. The silica and titanium dioxide nanoparticles were found in the placenta, fetal liver and fetal brain. Mice treated with these nanoparticles had smaller uteri and smaller fetuses than untreated controls. Fullerene molecules and larger (300 and 1,000 nm) silica particles did not induce these complications. These detrimental effects are linked to structural and functional abnormalities in the placenta on the maternal side, and are abolished when the surfaces of the silica nanoparticles are modified with carboxyl and amine groups.

Nanomaterials such as nanosilica particles (nSPs), titanium dioxide nanoparticles (nano-TiO_2) and carbon nanotubes are already being applied in electronics[1], foods[2], cosmetics[3] and drug delivery[4]. nSPs are used as additives in cosmetics and foods because they are highly hydrophilic, easy to synthesize and their surfaces can be modified easily[5,6]. The increasing use of nanomaterials has raised concerns[7–9] because of recent reports showing that carbon nanotubes can induce mesothelioma-like lesions in mice, similar to those induced by asbestos[10,11]. We have also shown that nSPs can induce severe liver damage in mice and inflammatory responses *in vitro*[12,13].

Fetuses are known to be more sensitive to environmental toxins than adults[14–16], and it has been suggested that many chemical toxins in air, water and foods can induce pregnancy complications in humans[15,16]. An estimated 1 to 3% of women in the USA suffer recurrent miscarriages[17] and 7–15% of pregnancies are affected by poor fetal growth (a condition known as intrauterine growth restriction, IUGR)[18]. IUGR, which refers to a fetus with a weight below the 10th percentile for its gestational age, can cause fetal death and predisposes the child to a lifelong increased risk for cardiovascular disorders and renal disease[19,20]. Examining the potential risk of nanomaterials for causing miscarriage and IUGR is therefore essential.

Although some studies have shown transplacental transport of nanomaterials in pregnant animals and nanomaterial-induced neurotoxicity in their offspring[21–26], the effects of nanomaterials on pregnant animals have not yet been studied. Here, we investigated the biodistribution and fetotoxicity of various sizes of surface-modified nSPs, fullerene C_{60} and nano-TiO_2 in pregnant mice. Our results indicate that nSPs with diameters less than 100 nm and nano-TiO_2 with diameters of 35 nm induce resorption of embryos and fetal growth restriction. Furthermore, we found that modifying the surface of nSPs from –OH to –COOH or $-NH_2$ functional groups can prevent these pregnancy complications. These data include basic information regarding possible ways of creating safer nanomaterials.

Biodistribution of nanoparticles

Silica particles are well suited for studying the influence of nanomaterial size on biodistribution and various biological effects because they show much better dispersibility in aqueous solutions than most other nanomaterials[27]. We used silica particles with diameters of 70 nm (nSP70), 300 nm (nSP300) and 1,000 nm (mSP1000) to study the effect of size on biodistribution of the particles in pregnant mice. Two other common nanomaterials, nano-TiO_2 and fullerene, were also examined. All silica nanoparticles were confirmed by transmission electron microscopy (TEM) to be smooth-surfaced spheres (Supplementary Fig. S1a,b,c,g,h,i)[12,13]. The hydrodynamic diameters of nSP70, nSP300, mSP1000, nano-TiO_2 and fullerene were 65, 322, 1,140, 217 and 143 nm, respectively, with zeta

[1]Department of Toxicology and Safety Science, Graduate School of Pharmaceutical Sciences, Osaka University, 1-6 Yamadaoka, Suita, Osaka 565-0871, Japan, [2]Laboratory of Biopharmaceutical Research, National Institute of Biomedical Innovation, 7-6-8, Saito-Asagi, Ibaraki, Osaka 567-0085, Japan, [3]The Center for Advanced Medical Engineering and Informatics, Osaka University, 1-6, Yamadaoka, Suita, Osaka 565-0871, Japan, [4]Department of Developmental Medicine, Osaka Medical Center and Research Institute for Maternal and Child Health, 840 Murodo-cho, Izumi, Osaka 594-1101, Japan, [5]Bioresources Research, Laboratory of Common Apparatus, National Institute of Biomedical Innovation, 7-6-8, Saito-Asagi, Ibaraki, Osaka 567-0085, Japan, [6]Vitamin C60 BioResearch Corporation, 1-3-19, Yaesu, Chuo-ku, Tokyo 103-0028, Japan, [7]Mitsubishi Corporation, 2-6-1, Marunouchi, Chiyoda-ku, Tokyo 100-8086, Japan, [8]Graduate School of Pharmaceutical Sciences, Kobe-Gakuin University, 1-1-3, Minatojima, Chuo-ku, Kobe, Hyogo 650-8586, Japan, [9]Department of Biomedical Innovation, Graduate School of Pharmaceutical Sciences, Osaka University, 7-6-8 Saito-asagi, Ibaraki, Osaka 567-0085, Japan, [10]Department of Obstetrics and Gynecology, University of Toyama, 2630, Sugitani, Toyama 930-0194, Japan; †These authors contributed equally to this work.
*e-mail: yasuo@phs.osaka-u.ac.jp; ytsutsumi@phs.osaka-u.ac.jp

potentials of −53, −62, −67, −23 and −13 mV, respectively (see Supplementary Fig S2 for the physicochemical properties of all the materials). The size distribution spectrum of each silica particle showed a single peak (Supplementary Fig. S1m), and the hydrodynamic diameter corresponded almost precisely to the primary particle size for each sample (Supplementary Figs S1m and S2), indicating that the silica particles used in this study were well-dispersed in solution.

We examined the relationship between particle size and biodistribution in the placenta by whole-body imaging analysis after intravenous injection (through the tail vein) of fluorescent DY-676-labelled nSP70, nSP300 or mSP1000 into pregnant mice at gestational day 16 (GD16). At 24 h post-injection, intense fluorescence was observed in the liver of all mice receiving the differently sized nanoparticles (Fig. 1a), suggesting that the accumulation of nanoparticles in the liver is independent of size. Fluorescence was seen in the placenta of mice treated with nSP70, but not in mice treated with nSP300 or mSP1000 (Fig. 1a). We confirmed that ~5% of fluorescent DY-676 dissociated from the silica particles after *in vitro* incubation in phosphate buffered saline (PBS) for 24 h at 37 °C (Supplementary Fig. S1n), and no fluorescence was detected in the placenta of mice treated with fluorescent DY-676 only (data not shown), indicating that the fluorescence observed in the mice was caused by silica particle accumulation in the tissues.

TEM analysis revealed that nSP70 (nanosized spherical black objects in Fig. 1b–g) were found in placental trophoblasts (Fig. 1b,c), fetal liver (Fig. 1d,e) and fetal brain (Fig. 1f,g). No particles were seen in the placenta, fetal liver or fetal brain of mice treated with nSP300 or mSP1000 (data not shown). These results suggest that the biodistribution of silica particles varied according to particle size, and that only the smaller nSP70 nanoparticles accumulated in the placenta and fetus. Similarly, nano-TiO_2 were found in placental trophoblasts (Fig. 1h,i), the fetal liver (Fig. 1j,k) and fetal brain (Fig. 1l,m) after intravenous injection into pregnant mice. We did not evaluate the biodistribution of fullerene C_{60} because of the difficulty in detecting fullerene using TEM.

Recently, several reports have shown that some nanomaterials can penetrate mouse and *ex vivo* human placental tissue[25,28], and it is generally known that high-molecular-weight species (>1,000 Da) do not penetrate the placenta by passive diffusion. Thus, we speculated that nSP70 either directly injured the blood–placenta barrier or was actively transported through it, or both. Furthermore, nSP70 in the fetal circulation would have access to the fetal liver and brain, because the development of the blood–brain barrier in the fetal brain is incomplete[29].

Fetotoxicity of nanoparticles

To determine the fetotoxicity of nSP70, nSP300, mSP1000, nano-TiO_2 and fullerene in pregnant mice, we intravenously injected the particles (100 μl, 0.8 mg per mouse) into pregnant mice on two consecutive days, at GD16 and GD17, and measured the maternal blood biochemistry. None of the silica particles induced any significant changes in the levels of aspartate aminotransferase (AST), alanine aminotransferase (ALT) and blood urea nitrogen (BUN), and all parameters remained within the physiological range, indicating that the particles did not induce maternal liver and kidney damage at the administered doses (Supplementary Fig. S3). Blood pressure and heart rates among all groups of mice that received silica nanoparticles were similar and comparable to control animals receiving PBS (Supplementary Fig. S4). However, there was a significant increase in the number of granulocytes in nSP70-treated pregnant mice compared with control mice receiving PBS (Supplementary Fig. S5).

When compared to control mice, the maternal body weight of nSP70- and nano-TiO_2-treated mice decreased at GD17 and GD18, whereas those treated with nSP300, mSP1000 and fullerenes did not show any changes (Fig. 2a). Mice that received nSP70 and nano-TiO_2 had 20% and 30% lower uterine weights (Fig. 2b,c), respectively, and significantly higher fetal resorption rates than control mice and those that received nSP300, mSP1000 particles or fullerene (Fig. 2d). nSP70- and nano-TiO_2-treated mice also had smaller fetuses (nearly 10% lower than control mice, Fig. 2e,g) and smaller amnion sacs than mice that received nSP300, mSP1000 or fullerene.

In contrast, the weights of placentae were the same among all groups of mice (Fig. 2f,h). When mice were injected with lower concentrations of nSP70 (0.2 and 0.4 mg per mouse), none of the above symptoms was observed; fetal resorption and growth restriction were seen only at the highest dose used (0.8 mg per mouse; Supplementary Fig. S6). These results indicate that only nSP70 at the highest concentration and nano-TiO_2 induced fetal resorption and restricted fetal growth; fullerene did not induce any pregnancy complications. The doses used here are typical of preclinical studies for drug delivery applications of silica particles, intravenously administered at several hundred milligrams per mouse[30]. In contrast, the most common route of nano-TiO_2 exposure to humans is through the skin (for example, through the application of nano-TiO_2-containing cosmetics) and some reports have suggested that nano-TiO_2 particles do not penetrate into living skin[31,32]. Therefore, we believe that nano-TiO_2 may not induce any pregnancy complications following topical application. Furthermore, we have confirmed that the nano-TiO_2 used in this study did not induce cellular toxicity and DNA damage *in vitro* (data not shown).

It is known that the surface properties of nanomaterials can influence biodistribution, inflammatory responses and cellular toxicity[27,33]. We examined the relationship between fetotoxicity and the surface properties of nSP70. The nSP70 was surface-modified with COOH or NH_2 functional groups (nSP70-C or nSP70-N, respectively), and both were confirmed by TEM to be smooth-surfaced spherical particles (Supplementary Fig. S1). The hydrodynamic diameters of the nSP70-C and nSP70-N were 70 and 72 nm, respectively, with zeta potentials of −76 and −29 mV, respectively, indicating that surface modification changed the surface charge of the particles (Supplementary Fig. S2).

As with nSP70, mice that were intravenously injected with DY-676-labelled nSP70-C and nSP70-N showed fluorescence in the placenta (Fig. 1a). TEM analysis revealed that nSP70-C and nSP70-N were found in placental trophoblasts (Fig. 1n,q), fetal liver (Fig. 1o,r) and fetal brain (Fig. 1p,s), indicating that the particles accumulated in the placenta and fetus. The maternal body weights of mice treated with nSP70-C or nSP70-N were the same as those observed for control mice (Fig. 2a). nSP70-C and nSP70-N did not affect the uterine weight (Fig. 2c), fetal weight (Fig. 2e,g) or fetal resorption rate (Fig. 2b,d). These results suggest that modifying the surface of nSP70 can prevent resorption and fetal growth restriction induced by nSP70.

Placental dysfunction in nSP70-treated mice

Normal placental development is required for embryonic growth, and placental dysfunction has been associated with miscarriage and fetal growth restriction[34,35]. The mature murine placenta consists of four layers: maternal decidua, trophoblast giant cell, spongiotrophoblast and labyrinth[34,35] (Fig. 3a). Maternal spiral arteries converge into canals between the trophoblast giant cells, and these canals pass through the spongiotrophoblast and labyrinth layers[34,35]. The exchange of respiratory gases, nutrients and waste takes place in the labyrinth layer between the fetal blood vessels and maternal blood sinuses[34,35].

To clarify the relationship between particle size, fetotoxicity and placental dysfunction, we examined the pathological histology of the placenta in nSP-treated mice using haematoxylin and eosin (H&E) staining (Fig. 3b–e). The placenta of mice treated with nSP70 showed variable structural abnormalities, whereas those treated